

Review

Application of Deep Learning in Blind Motion Deblurring: Current Status and Future Prospects

Yawen Xiang¹, Heng Zhou^{2,1}, Chengyang Li^{3,1}, Fangwei Sun¹, Zhongbo Li^{1,*} and Yongqiang Xie¹

¹ the Institute of Systems Engineering, Academy of Military Science, Beijing 100141, China

² the School of Electronic Engineering, Xidian University, Xi'an 710071, China;

³ the School of Electronics Engineering and Computer Science, Peking University, Beijing 100871, China;

* Corresponding author: Zhongbo Li

Abstract: Motion deblurring is one of the fundamental problems of computer vision and has received continuous attention. The variability in blur, both within and across images, imposes limitations on non-blind deblurring techniques that rely on estimating the blur kernel. As a response, blind motion deblurring has emerged, aiming to restore clear and detailed images without prior knowledge of the blur type, fueled by the advancements in deep learning methodologies. Despite strides in this field, a comprehensive synthesis of recent progress in deep learning-based blind motion deblurring is notably absent. This paper fills that gap by providing an exhaustive overview of the role of deep learning in blind motion deblurring, encompassing datasets, evaluation metrics, and methods developed over the last six years. Specifically, we first introduce the types of motion blur and the fundamental principles of deblurring. Next, we outline the shortcomings of traditional non-blind deblurring algorithms, emphasizing the advantages of employing deep learning techniques for deblurring tasks. Following this, we categorize and summarize existing blind motion deblurring methods based on different backbone networks, including convolutional neural networks, generative adversarial networks, recurrent neural networks, and Transformer networks. Subsequently, we elaborate not only on the fundamental principles of these different categories but also provide a comprehensive summary and comparison of their advantages and limitations. Qualitative and quantitative experimental results conducted on four widely used datasets further compare the performance of state-of-the-art methods. Finally, an analysis of present challenges and future pathways aims to guide and inspire researchers in the dynamic domain of image deblurring using deep learning techniques. This review aspires to serve as an invaluable reference for those immersed in this field of study. All collected models, benchmark datasets, source code links, and codes for evaluation have been made publicly available at <https://github.com/VisionVerse/Blind-Motion-Deblurring-Survey>

Keywords: Motion blur; Blind deblurring; Blind motion deblurring; Deep learning

Citation: Xiang, Y.; Zhou, H.; Li, C.; Sun, F.; Li, Z.; Xie, Y. Application of Deep Learning in Blind Motion Deblurring: Current Status and Future Prospects. *Remote Sens.* **2024**, *1*, 0. <https://doi.org/>

Received: January 10, 2024

Revised:

Accepted:

Published:

Copyright: © 2024 by the authors. Submitted to *Remote Sens.* for possible open access publication under the terms and conditions of the Creative Commons Attribution (CC BY) license (<https://creativecommons.org/licenses/by/4.0/>).

1. Introduction

Motion blur is a common artifact in images caused by the relative movement between the camera and the scene during the exposure [1,2]. This effect can cause object contours in the image to be blurred or stretched, thereby reducing the clarity and detail of the image and affecting various computer vision tasks such as autonomous driving [3,4], object segmentation [5,6] and scene analysis [7,8]. Understanding the origins of motion blur is critical to developing effective elimination strategies.

The blurry process, as a fundamental degradation model, can be depicted as the convolution between a clear image and a blur kernel [9–11]:

$$\mathbf{B} = \mathbf{S} \otimes \mathbf{k} + \mathbf{n}, \quad (1)$$

where \mathbf{B} and \mathbf{S} are the observed blurred image and sharp image, respectively. \mathbf{k} and \mathbf{n} represent the blur kernel and noise. \otimes is the convolution operation. When \mathbf{k} is known,

arXiv:2401.05055v1 [cs.CV] 10 Jan 2024



Figure 1. Sharp-blurry images.

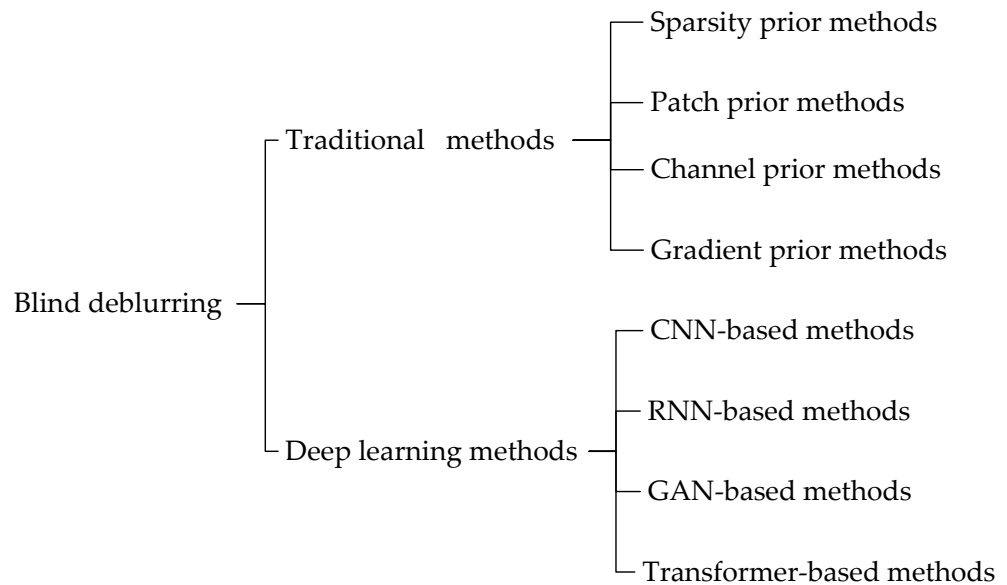


Figure 2. An overview of traditional and deep learning methods for blind motion deblurring.

the inverse process of this task is referred to as non-blind deblurring [12–14]. However, \mathbf{k} is often unknown when dealing with blurred images, leading to tasks known as blind deblurring [15–19].

Motion blur can be divided into two types: global motion blur and local motion blur. As shown in Figure 1 (b), global motion blur is caused by the shaking of the camera [20], resulting in consistent blurring across the entire image. As shown in Figure 1 (c), local motion blur occurs due to relative motion between the target object and the static background, resulting in blur [21].

Deblurring represents an ill-posed problem that cannot be directly solved. The traditional blind deblurring methods [22–24] start with the blur degradation model, employing mathematical modeling or convolutional networks to predict the blur kernel. Then they utilize the estimated blur kernel to restore the image through deconvolution. These approaches rely on prior knowledge of both the image and the blur kernel to address the ill-posedness in deblurring. As shown in the traditional method on Figure 2, the commonly used prior algorithms are sparsity prior [25–27], patch prior [28–30], channel prior [31–33], gradient prior [34–36] and so on. The quality of image deblurring is ensured by the priori algorithms. These traditional methods heavily rely on blur kernel estimation, and the effectiveness of the deblurring process directly depends on the accuracy of the kernel estimation. However, in complex real-world scenarios, the blur kernel in the blurring process tends to be complex, variable, and difficult to parameterize, causing the traditional methods to often perform inadequately.

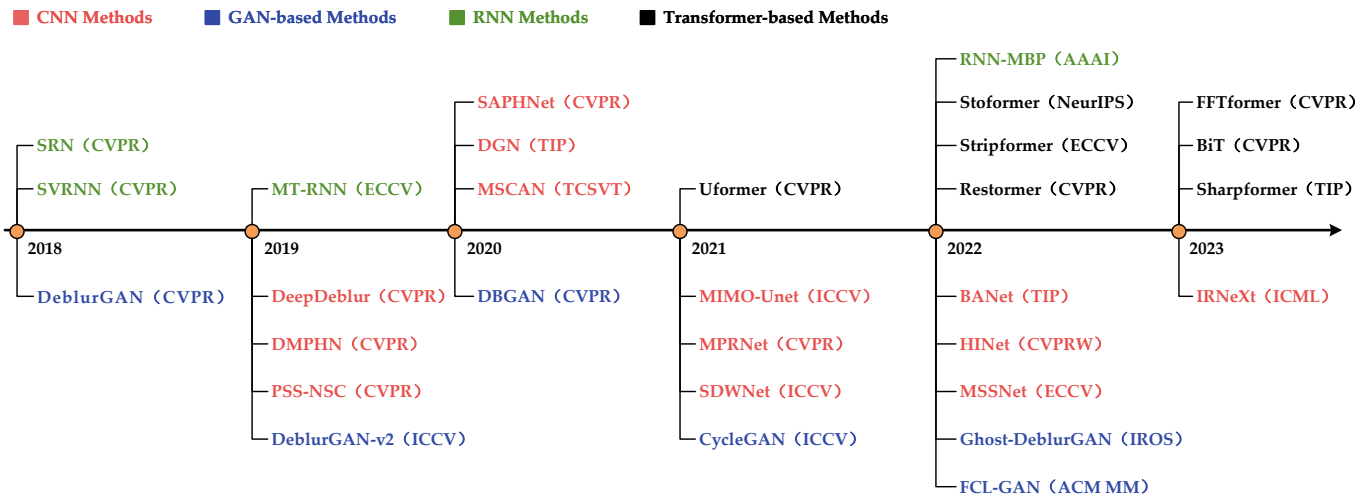


Figure 3. Overview of deep learning methods for blind motion deblurring.

In recent years, deep learning technology has developed rapidly and has been widely applied in image processing [37,38]. Deep learning-based methods have powerful feature learning and mapping capabilities, allowing them to learn complex patterns of blur removal from extensive datasets [39]. Consequently, significant progress has been made in image deblurring[40–44] As depicted in Figure 3, existing blind motion deblurring methods can be categorized based on different backbone networks, namely: convolutional neural networks (CNN) [45], generative adversarial networks (GAN) [46,47], recurrent neural networks (RNN) [48], and Transformer networks [49]. The deep learning methods can adaptively learn the blur features according to the training data, thus achieving end-to-end image deblurring. They can directly generate sharp images from blurred ones, which improves the effect of image deblurring. Compared to the traditional methods, the deep learning methods [50–52] demonstrate improved robustness in real-world scenarios and possess broader applicability.

In this paper, we focus on the application of deep learning in blind motion deblurring. Overall, the main contributions of this paper are as follows:

- In this review, we comprehensively overview the research progress of deep learning in blind motion deblurring, encompassing the causes of motion blur, blurred image datasets, evaluation metrics for image quality, and methods developed over the past six years.
- Specifically, we introduce a classification framework for blind motion deblurring tasks based on backbone networks, categorizing existing methods into four classes: CNN-based, RNN-based, GAN-based, and Transformer-based approaches.
- Furthermore, for each type of blind motion deblurring method, we provide an in-depth summary of their fundamental principles, analyzing the advantages and limitations of each approach. Qualitative and quantitative experimental results on four widely used datasets further showcase the performance differences among different blind motion deblurring methods.
- Finally, we conduct a prospective analysis and summary of current research challenges and potential future directions in blind motion deblurring. This review aims to offer researchers and practitioners in the field a comprehensive understanding and a valuable reference for further advancements.

The subsequent sections of this paper are structured as follows: We first summarized the classification and research status of image blind motion deblurring methods in Sec. 2. Then, We briefly introduced the public datasets and evaluation metrics in Sec. 3. Next, Sec. 4 describes the basic principles of different types of methods in detail, and summarizes and compares the advancements and shortcomings of different methods. Qualitative and

quantitative experimental results on four common datasets further compare the performance of different methods. Finally, in Sec. 5 and Sec. 6, we provide a prospective analysis of current research challenges and potential future directions in blind motion deblurring.

2. Deep Learning Methods for Blind Motion Deblurring

As shown in Figure 3, the foundational framework of deep learning-based image deblurring methods can be divided into four categories: CNN-based, RNN-based, GAN-based, and Transformer-based image deblurring methods. We discuss these methods in the following sections.

2.1. CNN-based Blind Motion Deblurring Methods

CNN-based image blind deblurring methods can be divided into two categories according to the process of image deblurring. One is the early two-stage image deblurring network shown in Figure 4 (a), and the other is the end-to-end image deblurring methods with the better performance shown in Figure 4 (b).

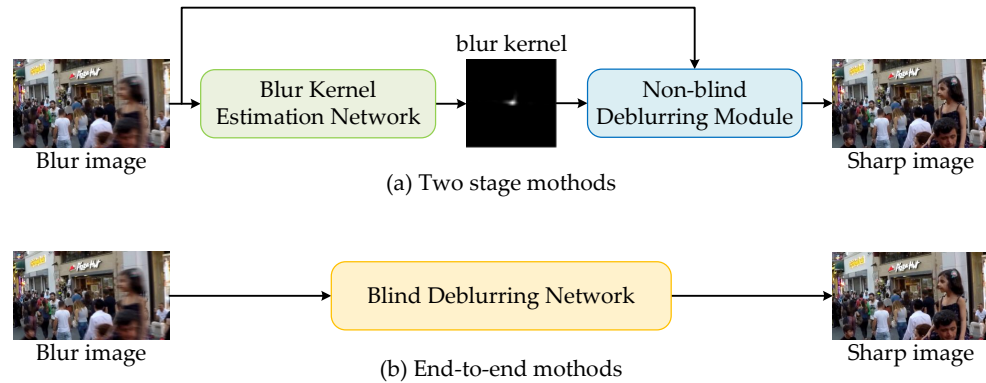


Figure 4. Two CNN-based blind motion deblurring frameworks.

2.1.1. Two-stage CNN-based Blind Motion Deblurring Methods

Early image blind deblurring methods are mainly for deblurring a single blur kernel image. The process of image deblurring was divided into two stages, as shown in Figure 4 (a). The first stage is estimating the blur kernel through a neural network. Then, the estimated blur kernel is used for deconvolution or inverse filtering operations on the blurred image to achieve the effect of image deblurring.

Classical methods such as: Schuler et al. [53] trained a blind image deconvolution network to deblur the image. This network primarily consists of three parts: a feature extraction module, a blur kernel estimation module, and an image estimation module. The estimated blur kernel from the blur kernel estimation module is used to iteratively update the deblurred image. Sun et al. [54] proposed to estimate the heterogeneous motion blur through the CNN model and then deconvolute the blurred images, which can effectively estimate the spatially varying motion kernel and achieve a better effect of removing motion blur. To address the issue of the non-uniform blur, Cronje et al. [55] proposed a CNN-based image deblurring method. This method trained two CNN networks, one for estimating the vector of non-uniform motion and the other for image deconvolution. It accurately estimated non-uniform blur and enhanced the effectiveness of image deblurring. Ayan Chakrabarti et al. [56] trained a neural network for estimating the blur kernel of blur images. Using the estimated single global blur kernel, they used non-blind deconvolution to obtain deblurred images. Gong et al. [57] trained a fully convolutional neural network for estimating image motion flow. Then they performed non-blind deconvolution to recover clear images from the estimated motion flow. This method avoids the iterative process of underlying image priors. Xu et al. [58] proposed a deep convolutional neural network to extract sharp edges from blur images for kernel estimation, which does not require any

coarse-to-fine strategy or edge selection, thus greatly simplifying the kernel estimation and reducing the computational amount. Kaufman et al. [59] analyze the blurring kernel by applying convolutional layers and pooling operations to extract features at multiple scales. Subsequently, the estimated kernel, along with the input image, is fed into a synthetic network to perform non-blind deblurring.

These two-stage image deblurring methods rely too much on the blur kernel estimation of the first stage, and the estimated blur kernel quality is directly related to the effect of image deblurring. In reality, the blur is mostly uneven, and the size and direction of the blurred image are also uncertain. So in the real scenes, this method can not remove complex real blur very well.

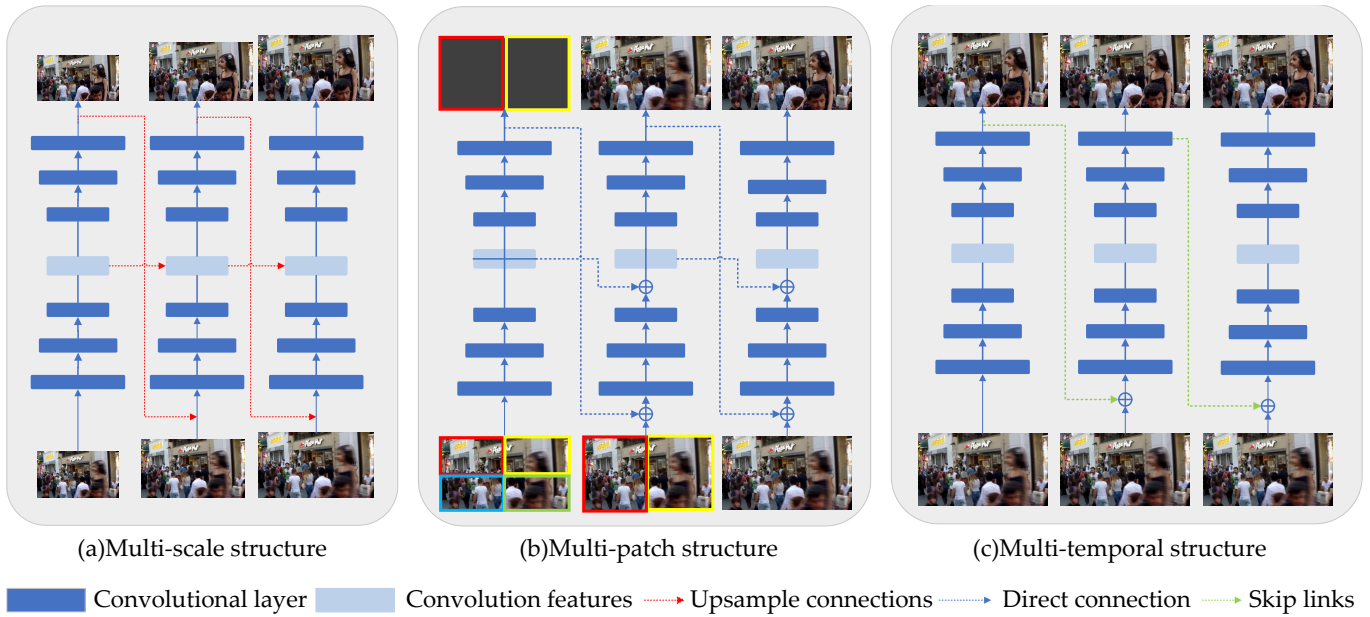


Figure 5. Different end-to-end CNN-based blind motion deblurring network architectures.

2.1.2. End-to-end CNN-based Blind Motion Deblurring Methods

The end-to-end image deblurring method generates a clear image directly from the input blurred image. It utilizes neural networks to learn complex feature mapping relationships for better restoration of clear images. End-to-end image deblurring algorithms have made significant progress since Xu et al. [60] first implemented end-to-end motion blur image restoration using CNNs. As shown in Figure 5, CNN-based end-to-end image deblurring methods can be categorized into three types: multi-scale, multi-patch, and multi-temporal structures.

Multi-scale Structure: As shown in Figure 5 (a), the multi-scale model extracts multi-scale feature information from blurry images. Based on this extracted information, it progressively restores the image from coarse to fine levels. In order to better handle non-uniform blur in dynamic scenes, Nah et al. [61] proposed a multi-scale convolutional neural network for end-to-end restoration of blurred images. Following a similar approach, many subsequent researchers have improved on the multi-scale strategy to obtain better results [62–65]. However, its limitation lies in scaling the blurred image to a lower resolution, often resulting in the loss of edge information. Overlaying multi-scale input images onto sub-networks gradually enhances image clarity from lower-level to higher-level sub-networks, inevitably incurring higher computational costs. To reduce the spatio-temporal complexity of employing a multi-scale strategy network, Cho et al. [66] devised a network architecture that starts from coarse to fine, proposing a multi-input multi-output U-Net network. This approach allows for a better execution of deblurring from coarse to fine.

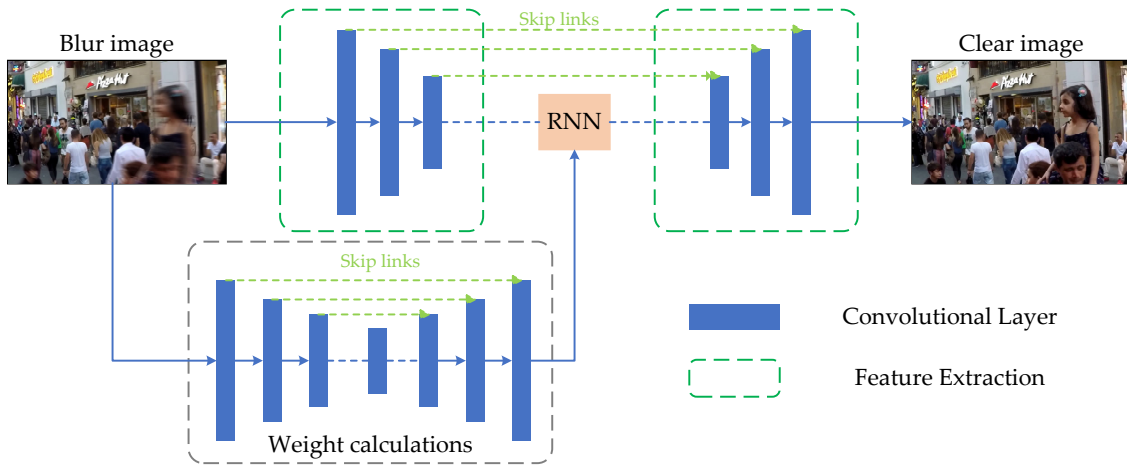


Figure 6. A spatial variant RNN image deblurring method.

Multi-patch Structure: As shown in Figure 5 (b), the multi-patch structure segments the blurred input into multiple patches for prediction. Inspired by spatial pyramid matching, Zhang et al. [67] proposed a deep hierarchical end-to-end CNN model called DMPHN. This model used multiple patches for a fine-to-coarse operation to handle blurry images. To remove spatially varying blur, Suin et al. [68] proposed a patch hierarchical attention architecture. It significantly enhances deblurring effects through effective pixel-wise adaptation and feature attention. Building upon DMPHN, Zhang et al. [69] proposed a self-supervised event-guided deep hierarchical multi-patch network, which handles blurry images through a layered representation from fine to coarse. By stacking patch networks to increase network depth, this model enhanced deblurring performance. However, when segmenting input or features, discontinuities in contextual information may arise, potentially generating artifacts and leading to suboptimal image deblurring in dynamic scene contexts [70].

Multi-temporal Structure: As shown in Figure 5 (c), the multi-temporal structure gradually eliminates non-uniform blur over multiple iterations. The multi-temporal framework [71] was introduced to handle non-uniform blur and exhibited significant performance improvements. However, rigid progressive training and inference processes might not adapt well to images with varying degrees of blur in different regions. Subsequent researchers have proposed numerous time-series-based deblurring methods, learning from different temporal scales of motion blur to achieve enhanced deblurring effects [72,73].

2.2. RNN-based Blind Motion Deblurring Methods

Recurrent Neural Networks (RNNs) are commonly used for handling sequential data such as text, language, and time series, demonstrating exceptional performance when dealing with data that exhibit temporal or sequential patterns [74]. Due to their memory-based neural network architecture, RNNs have found applications in image processing as well. For instance, Zhang et al. [48] proposed an end-to-end spatially variant RNN network for deblurring in dynamic scenes. As illustrated in Figure 6, the weights of RNNs are learned by deep CNNs. They analyzed the relationship between spatially variant RNNs and the deconvolution process, demonstrating the ability of spatially variant RNNs to simulate the deblurring process. Models trained using the proposed RNNs are notably smaller and faster. To better utilize the properties of spatially varying RNNs, Ren et al. [75] extend a unidirectionally connected one-dimensional spatially varying RNN to a two-dimensional spatial RNN with three-way connectivity. 2D RNNs can capture a larger receptive field and learn denser propagation between neighboring pixels compared to 1D RNNs, further improving deblurring performance. Tao et al. [63] proposed a multi-scale deep neural network for single image deblurring based on convolutional long short-term memory (Conv LSTM), effectively utilizing previous frames and image features. Dongwon Park et al. [71] developed a multi-temporal recurrent neural network (MT-RNN) based on

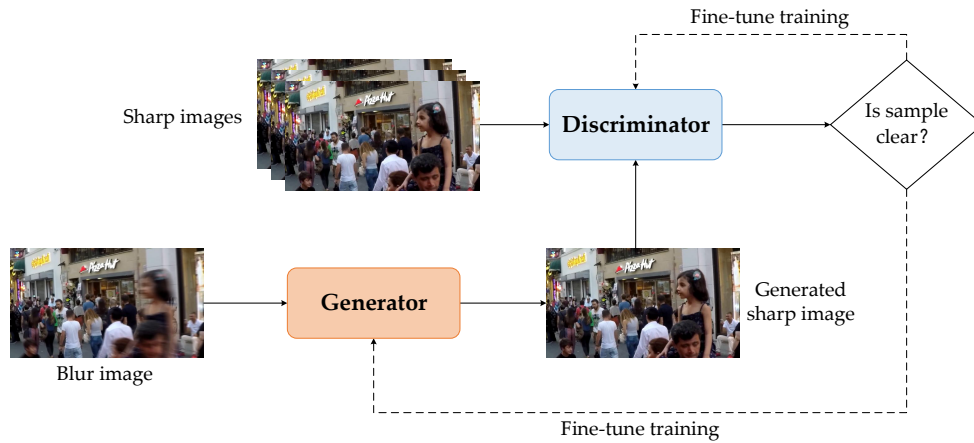


Figure 7. GAN-based deblurring algorithm flow.

recursive feature mapping for blind single-image deblurring, progressively deblurring a single image in an iterative process. In practical applications, CNNs and other models are often combined with RNNs to compensate for certain limitations in image processing, such as sequence length restrictions and computational complexity.

2.3. GAN-based Blind Motion Deblurring Methods

With GANs [46] showing promising results in computer vision tasks, they have also been applied to image deblurring tasks. The basic process of image deblurring based on GANs is illustrated in Figure 7. The generator learns to restore clear images from blurry ones, while the discriminator assesses whether the generated clear images are real, providing feedback to adjust the training of both the generator and discriminator.

Ramakrishnan et al. [76] proposed a depth filter based on GAN. For better restoration performance, it combines global jump connections and dense structure. Additionally, the model omits the blur kernel estimation process, significantly reducing the testing time required for practical applications. Lin et al. [77] proposed an adversarial blurred region mining and refinement method. This method can drive CGAN [78] to learn real sharp image distributions globally and locally for blind image deblurring. Based on GANs, O.Kupyn et al. [79] proposed an end-to-end image deblurring network termed *deblurGAN*. *DeblurGAN* was trained based on WGAN [80] with gradient penalty [81] and perceptual loss [82], achieving notable deblurring effects. Based on *DeblurGAN*, O. Kupyn et al. [83] proposed *DeblurGAN-v2*. This model incorporates a feature pyramid network within the generator. The discriminator employs a relativistic discriminator and uses least squares loss to assess the generated images on both global and local scales. Moreover, recognizing the impact of backbone network selection on deblurring quality and efficiency, *DeblurGAN-v2* utilizes an embedded architecture that allows the use of different backbone networks for feature propagation. Compared to *DeblurGAN*, *DeblurGAN-v2* demonstrates significant improvements in both performance and efficiency. Peng et al. [84] also proposed the *MobileNetDeblur-GAN (MND-GAN)* deblurring algorithm based on the *DeblurGAN* algorithm. This algorithm utilizes *MobileNet* as a feature extractor to build a feature pyramid network. Additionally, it employs a multi-scale discriminator to jointly train the generator, reducing the computational cost of the generator while ensuring deblurring quality.

To further enhance image deblurring performance, Zhang et al. [85] proposed a multi-scale deblurring network based on GANs. The model first restores the edge information of the blurred image and then utilizes clear edges to guide a multi-scale network for image deblurring. Starting from the blurry images themselves, Zhang et al. [86] proposed an image deblurring approach that combines two GAN models: a BGAN subnetwork for learning the image blurring process to generate motion-blurred images and a DBGAN for

learning the restoration of motion-blurred images. By learning how to blur images, this method can better remove blurriness.

Supervised learning relies on a large amount of training data, but in reality, there are few real blurred-clear image pairs available for collection. Madam et al. [87] proposed an unsupervised motion image deblurring method based on GANs. The model employs GANs to learn the mapping relationship from blurred images to clear images. To prevent mode collapse and maintain consistency between deblurred and clear image gradients, the model incorporates a deblurring CNN module and a gradient module to constrain the solution space and guide the deblurring process. GAN-based methods may encounter issues during training such as model collapse and gradient disappearance [88], potentially resulting in artifacts and loss of details in the reconstructed images. Building upon the cycle-consistent generative adversarial network (CycleGAN) [89], Wen et al. [90] proposed an unsupervised image deblurring method using a multi-adversarial optimization CycleGAN to address artifacts in high-resolution image generation. This method iteratively generates clear high-resolution images through multiple adversarial constraints. Considering the significant role of edge restoration in the structure of deblurring blurry images, this method introduces a structural-aware strategy. It utilizes edge information to guide the network in deblurring, enhancing the network's ability to recover image details. Zhao et al. [91] introduced a contrast-guided multi-attention CycleGAN unsupervised algorithm for motion deblurring. It improved the deblurring performance of unsupervised algorithms. Lu et al. [92] proposed an unsupervised method for single image deblurring without pairing training images termed UID-GAN. The method introduces a disentangled framework to split the content and blur features of blurred images, which improves the deblurring performance.

Due to the current drawbacks of unsupervised learning, such as large model sizes, lengthy inference times, and strict constraints on image resolution and domains, Zhao et al. [93] proposed an unsupervised blind image deblurring model termed frequency-domain contrastive loss constrained lightweight CycleGAN (FCL-GAN). It designed lightweight domain transformation units and parameter-free frequency domain contrast units to ensure the algorithm's "lightweight" and "real-time" operation, overcoming the limitations of the generally large models and complex inference in unsupervised methods. Additionally, this model enhanced deblurring performance by introducing frequency-domain contrastive learning. Considering the practical application of image deblurring algorithms in real-world scenarios, Liu et al. [94] proposed a lightweight generative adversarial network termed Ghost-DeblurGAN. While this algorithm may not reach the advanced levels of deblurring, its advantage lies in its small model size and short inference time.

2.4. Transformer-based Blind Motion Deblurring Methods

The Transformer, renowned for its powerful attention mechanism, utilizes self-attention (SA) to capture long-range dependencies among patches in image sequences and adaptability to given input content [95–98]. When applied in image deblurring, it can achieve significant improvements in deblurring effectiveness.

Wang et al. [99] proposed an efficient and effective Transformer-based image restoration architecture called U-former by embedding local enhancement window Transformer blocks into a U-shaped structure [100]. They inserted learnable multi-scale restoration modulators into their decoder to enhance the quality of image restoration. The basic architecture is depicted in Figure 8. Although Uformer has shown promising performance in image restoration tasks, the heavy computation involved in self-attention restricts the application of the transformer within the encoding-decoding framework to limited depths. This inevitably affects the effectiveness of image restoration. Building upon U-former, Feng et al. [101] proposed a deep encoder-decoder image restoration network called U2-former, with Transformer as the core operation. This model employs two nested U-shaped structures to facilitate feature mapping at different scales, resulting in an enhanced image deblurring effect. To optimize computational efficiency, the model utilizes a feature filtering mechanism to discard low-quality features, thereby reducing unnecessary computations.

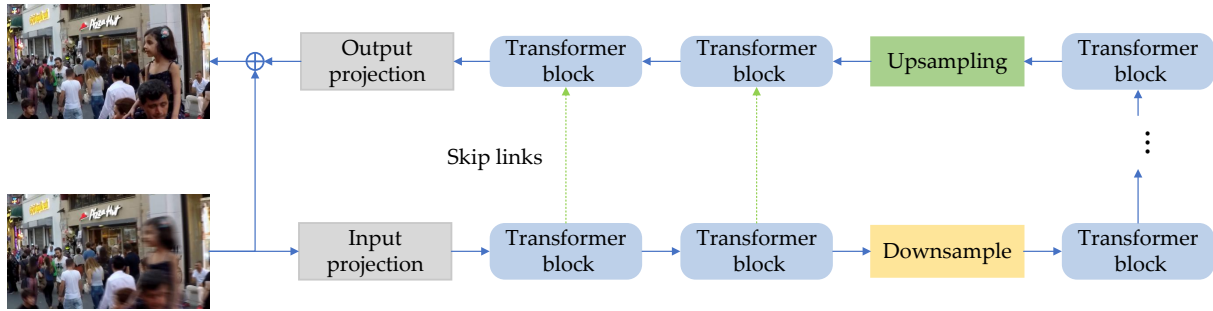


Figure 8. The Transformer-based deblurring network architecture.

To effectively eliminate non-uniform blur, Tsai et al. [102] proposed an efficient Transformer-based image deblurring algorithm termed Stripformer. This method reweights image features by computing intra-band and inter-band attention to address blur of different sizes and orientations. It achieves notable deblurring results without requiring extensive training data, enhancing the removal of non-uniform blur. Zamir et al. [103] proposed a Transformer-based image restoration network termed Restormer. This method employs a multi-head attention mechanism for feature fusion to handle high-resolution images in image restoration tasks. Additionally, this method utilizes multi-scale local-global representation learning to effectively utilize distant contextual information. It simultaneously reduces computations while enhancing the effectiveness of image restoration. Kong et al. [104] proposed an asymmetric network based on an encoder-decoder architecture. They designed an effective frequency-domain self-attention solver in the decoder, reducing spatial complexity and computational demands through element-wise operations. Additionally, they employed a discriminative frequency-based feedforward network (DFFN) to discern which low-frequency and high-frequency feature information should be retained for potential clear image restoration. Recently, Zhong et al. [105] proposed a Blur Interpolation Transformer (BiT) to reveal potential temporal correlations in blurry encodings. Based on multi-scale residual Swin Transformer blocks, they introduced dual-ended temporal supervision and a time-symmetric integration strategy to generate effective time-varying motion-rendered features, effectively generating clear image sequences from blurry inputs. Zou et al. [106] explored the significant roles of edges and textures in image deblurring and proposed a method called Edgeformer. This method utilizes edge information to enhance the correlation between pixels. By employing an edge-enhanced feed-forward network, it distinguishes between edge and texture features, resulting in improved image deblurring. To fully leverage both local and non-local features in images, Wu et al. [107] introduced the hierarchical pyramid attention transformer (HPAT) network, based on a transformer-based multi-level network structure. It employs hierarchical attention fusion modules (HAFM) to extract global contextual information, enhancing the feature representation capability. Using a fusion feed-forward neural network (F3N) for feature fusion has improved the deblurring effectiveness. Liang et al. [108] used deep features extracted from pre-trained visual transformers (ViT) [109] to encourage the recovered image to become clear without sacrificing quantitative performance. They also proposed local MAE perceptual loss and global distribution perceptual loss to guide image deblurring.

The existing image deblurring methods mainly focus on global deblurring, which may affect the clarity of locally blurred images. Li et al. [110] proposed a local dynamic motion deblurring transformation network (LDM-ViT) based on adaptive window pruning transformer blocks (AdaWPT). In order to focus the network attention on localized blur regions, AdaWPT removes unnecessary windows. Only the blurred regions are allowed to participate in the deblurring process, reducing the amount of unnecessary computation. Additionally, using labeled local blur image datasets to train the predictor can be able to remove local motion blur effectively. Yan et al. [111] introduced a Transformer-based dynamic scene image deblurring network called SharpFormer. They designed a Local-preserving

Transformer block (LTransformer) that learns local features while retaining global representations. To effectively apply LTransformer blocks to mid-resolution features, they used dynamic convolution blocks to adaptively handle input non-uniform blur, enhancing the quality of deblurred images.

2.5. Advantages and limitations of the four architectures.

In image deblurring, the four architectures CNN, RNN, GAN, and Transformer have their own advantages and limitations:

CNN is widely used in image processing to capture local features and spatial information [118,119]. Trained with large-scale datasets, CNN-based deblurring methods perform high efficiency and generalization capabilities in Table 2. The CNN structure is simple and suitable for image denoising and deblurring tasks [120]. However CNN-based methods may be limited by a fixed-size receptive field and may not be effective for image-deblurring tasks that deal with global information or long-range dependencies. In order to solve the problem of a limited receptive field, the more widely used method is to use dilated convolution.

As shown in Table 2, RNN applies to sequence data and can capture temporal or sequential dependencies, which may be useful in certain image sequence deblurring scenarios. There may be gradient vanishing or explosion problems when dealing with long-term dependencies [121]. Moreover, for image deblurring tasks, RNN is not well suited to capture spatial information [75]. Therefore, RNNs are generally combined with other structures to accomplish image deblurring tasks.

GAN improves the realism of image generation using adversarial training, which helps to generate more realistic deblurred images in Table 2. However, the training process may be unstable, requiring a balance between generator and discriminator training [122]. There may also be pattern crashes or non-convergence of training patterns.

As listed in Table 2, Transformer is able to capture global information and solve the remote spatial dependence problem [111], and has advantages in processing for some image tasks that require long-distance dependence. However, the image deblurring task involves the processing of a large number of pixels and has a high computational cost.

3. Datasets and Evaluation Metrics

3.1. Datasets

Most neural network-based image deblurring methods typically require paired images for training. Existing blurry image datasets can be roughly divided into two categories: synthetic datasets and real datasets. Synthetic datasets include the Köhler dataset, Blur-DVS dataset, GoPro dataset, and HIDE dataset, among others. Real image datasets comprise the RealBlur dataset, RsBlur dataset, ReLoBlur dataset, and so on. As shown in Figure 9, these are example images from some commonly used datasets. Table 1 summarizes and outlines

Table 1. Representative benchmark datasets for evaluating single image deblurring algorithms.

Real/Syn.	Dataset	Generative approach	Sizes	Train/Valid/Test
Synthetic	Köhler at al. [112]	Motion trajectory captured by 6D camera	4 sharp+48 blur	Not divided
	GoPro [61]	averaging over consecutive clear frames	3,214 pairs	2,103 / 0 / 1,111
	HIDE [113]	averaging over consecutive clear frames	8,422 pairs	6,397 / 0 / 2,025
	Blur-DVS [114]	averaging over consecutive clear frames	2178 pairs	1782 / 0 / 396
Real	RealBlur [115]	blurred images: Low shutter speed cameras clear images: High shutter speed cameras	4,738 pairs	3,758 / 0 / 980
	RsBlur [116]	blurred images: The long exposure camera clear images: the short exposure camera	13,358 pairs	8,878 / 1,120 / 3,360
	ReLoBlur [117]	blurred images: The long exposure camera clear images: short exposure time camera	2,405 pairs	2,010 / 0 / 395

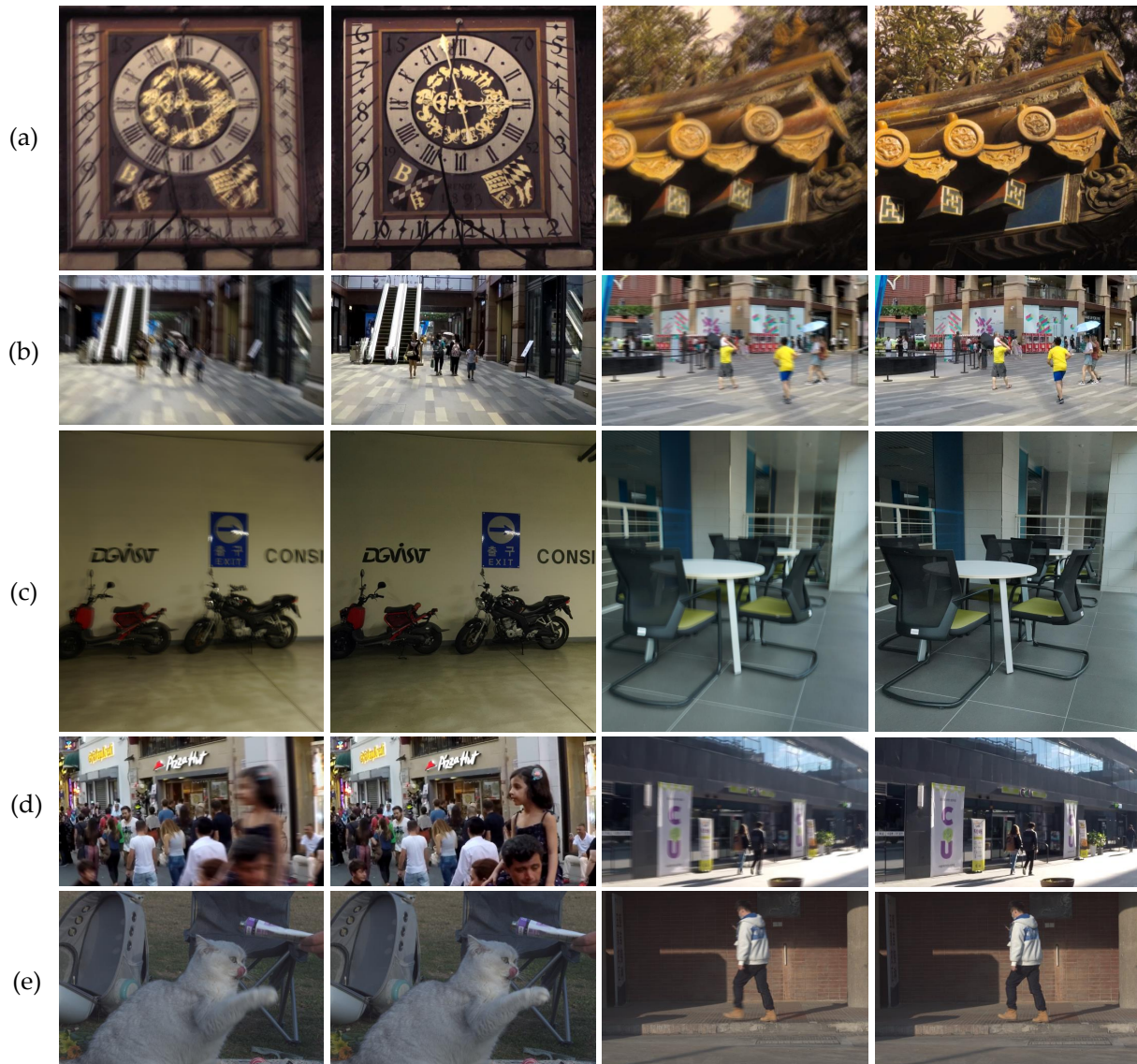


Figure 9. Some example images from (a) Köhler dataset, (b) HIDE dataset, (c) RealBlur-J dataset, (d) GoPro dataset, (e) ReLoBlur dataset.

the basic information of select datasets. We additionally provide bar graphs to compare the size of the datasets, as shown in Figure 10.

Köhler et al. Dataset: To simulate real camera shake, Köhler et al. [112] used a Stewart platform with six degrees of freedom to replay the camera’s motion trajectory. During the replay of the motion trajectory, a series of clear images and long-exposure blurry images were captured. The dataset comprises 4 clear images and 48 corresponding blurry images for 12 motion trajectories.

Blur-DVS Dataset: Created by Jiang et al. [114] using the DAVIS240C camera. The creation process involved capturing an image sequence with a slow-motion camera and then synthesizing 2,178 pairs of blurred and clear images by averaging adjacent 7 frames. The dataset consists of 1,782 pairs for training and 396 pairs for testing. Additionally, the dataset provides 740 real blurry images without paired clear images.

GoPro Dataset: Developed by Nah et al. [61], this dataset is one of the most commonly used deep learning methods. The dataset’s motion-blurred images are generated by integrating multiple instantaneous clear images within a time interval. Using a GoPro Hero4 Black camera capturing clear images at 240fps, they averaged over varying time windows to create blurred images, with the clear image at the window’s center serving as

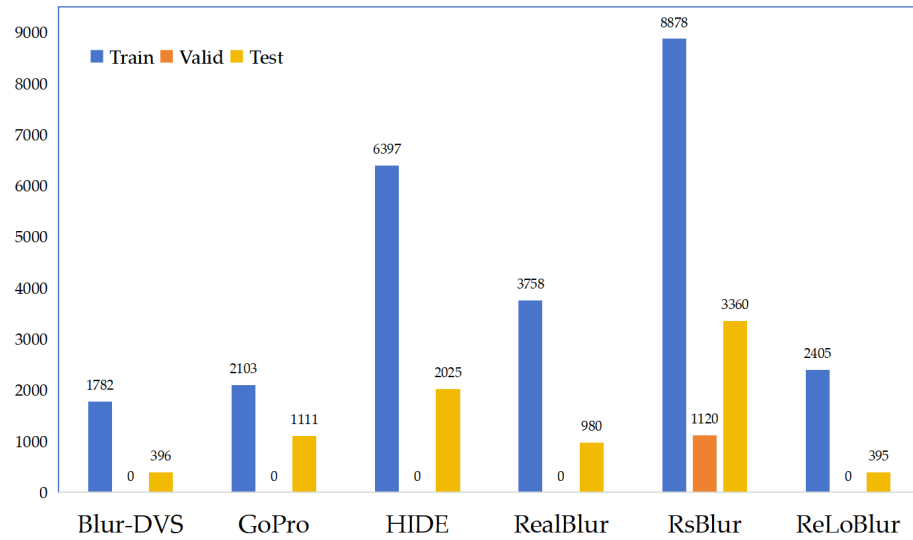


Figure 10. Histogram of the number of samples in the datasets.

the ground truth. It includes 3,214 pairs of clear and blurred images, divided into 2,103 pairs for training and 1,111 pairs for testing.

HIDE Dataset: Introduced by Shen et al. [113], this dataset focuses on motion blur in pedestrian and street scenes, including camera shake and object movement. The dataset was created by capturing videos at 240 fps using a GoPro Hero camera and then averaging frames from these high-frame-rate videos. They averaged 11 consecutive frames to generate blurred images and kept the center frame as the clear image. It comprises 8,422 clear-blurred image pairs, divided into 6,397 pairs for training and 2,025 pairs for testing.

RealBlur Dataset: Rim et al. [115] created the RealBlur dataset to train and test deep deblurring methods on real blurry images. The dataset consists of two subsets sharing the same image content. One subset, RealBlur-J, is generated from the camera's raw images, while the other, RealBlur-R, is generated from JPEG images processed by the camera's ISP. It contains a total of 9,476 image pairs, with each subset offering 4,556 pairs of blurry and ground truth clear images for 232 low-light static scenes. The blurry images in the dataset are affected by camera shake and were captured in low-light scenarios such as night streets and indoor rooms, covering common motion blur scenes.

RsBlur Dataset: Developed by Jaesung Rim et al. [116], the RsBlur dataset provides real blurry images of various outdoor scenes, each paired with a series of 9 clear images. It comprises 13,358 real blurry images from 697 scenes. For analysis, the dataset is divided into training, validation, and testing sets, containing 8,878, 1,120, and 3,360 blurry images, respectively, with 465, 58, and 174 scenes in each set.

ReLoBlur Dataset: Designed by Li et al. [117], ReLoBlur uses a simultaneous multi-band shutter device to capture local motion-blurred images along with their corresponding clear images, followed by post-processing for correction. Unlike synthetic blur datasets, ReLoBlur authentically showcases the mixing effect between locally moving objects and backgrounds, including overexposed, dimly lit real-life scenes, and complex blurred edges. It contains common real-life scenes such as pedestrians, vehicles, family members, pets, balls, plants, and furniture, among others. The dataset publicly provides 2,010 pairs of training set images and 395 pairs for testing. Additionally, the authors annotated the areas of local motion blur.

Table 2. A review of deep learning based deblurring methods, including publication information, overview, advantages and limitations.

Methods	Pub.	Category	Overview	Advantages	Limitations
DeepDeblur [61]	CVPR 2017	CNN	Removing complex motion blur from coarse to fine using a multi-scale recurrent network	End-to-end removal of complex motion blur without the need for kernel estimation	The mode has a large number of parameters, making training difficult
DMPHN [67]	CVPR 2019	CNN	Estimated by segmenting the image into multiple blocks and then removing blur at different scales	Overcoming the limitations of depth deblurring models on superposition depths	Feature segmentation may lead to discontinuous contextual information
PSS-NSC [123]	CVPR 2019	CNN	Multi-scale CNN deblurring networks are analyzed and a parameter-selective sharing scheme is proposed	Selective parameter sharing can improve the learning efficiency and generalization of the model	The introduction of new network structures and hopping connection mechanisms may have increased computational costs
DGN [124]	TIP 2020	CNN	An effective depth-guided network consisting of an image deblurring branch and a depth refinement branch is proposed	The use of depth maps allows for a better understanding of scene changes and facilitates the use of depth information	Deblurring quality depends on the accuracy and quality of the depth map
MSCAN [125]	TSCVT 2020	CNN	A multi-scale channel attention network is proposed for more robust feature representation and higher quality image recovery	Further taking advantage of multi-scale models, codec modules and residual block structures	The model has many parameters and is difficult to train
SDWNet [126]	ICCV 2021	CNN	A network structure combining extended convolution and wavelet reconstruction is proposed for image deblurring	Dilated convolution results in a larger perceptual field and reduces the loss of texture information during sampling	Introduction of wavelet transform increases the complexity of the network
MIMOU-Net [66]	ICCV 2021	CNN	Introducing asymmetric feature fusion for gradual recovery of clear images by coder-decoder	Handling multi-scale blurry with low computational complexity	Improvement of deblurring accuracy increases computational effort and time consuming

Table 2. A review of deep learning based deblurring methods, including publication information, overview, advantages and limitations.

Methods	Pub.	Category	Overview	Advantages	Limitations
MPRNet [70]	CVPR 2021	CNN	Multi-stage architecture, injecting supervision at each stage to incrementally improve degraded inputs	Horizontal connections exist between feature processing blocks to avoid information loss	High dependence on computing power
MSSNet [127]	ECCV 2022	CNN	A deep learning-based multi-scale stage network from coarse to fine is proposed	Multi-scale stage configurations and inter-scale information propagation contribute to the network's deblurring performance	Hyperparameter adjustment is more complex
HINet [128]	CVPRW 2022	CNN	Propose semi-instantiation to one piece using multi-stage architecture for image recovery task	HINet architecture generalizes well and has short inference time	Requires a large number of image pairs for training
BANet [129]	TIP 2022	CNN	Localization of blur direction and size by blurry perception for adaptive blur removal	Short inference time can well support subsequent real-time applications	Large amounts of diversity data are needed for training to adapt to dynamic scene blurring
IRNeXt [130]	ICML 2023	CNN	Integration of multi-stage mechanisms into a u-shaped network to remove different sizes of blur in a coarse-to-fine manner	The local attention module improves restoration quality by weighting high-frequency information	The performance improvement of deblurring depends on the number of MSM branches
SVRNN [48]	CVPR 2018	RNN	End-to-end trainable spatially-variant RNN for dynamic scene deblurring	The pixel-by-pixel weights of the RNN are learned by the deep CNN, which helps to remove blurring	Need for a larger feeling field, dealing with large areas and spatial variations
SRN [63]	CVPR 2018	RNN	Blur removal is achieved using a decoder with skip connections and parameter sharing across three scale	Sharing network weights at different scales, thus significantly reducing training complexity	Ignoring the variations between feature scales can easily saturate the network's performance

Table 2. A review of deep learning based deblurring methods, including publication information, overview, advantages and limitations.

Methods	Pub.	Category	Overview	Advantages	Limitations
MT-RNN [71]	ECCV 2019	RNN	Gradual removal of non-uniform blurring over multiple iterations using a self-looping MT structure	Contextual information is continuous, which facilitates the handling of blurring in dynamic scenes	Inflexible progressive training may not remove non-uniform blurring very well
DeblurGAN [79]	CVPR 2018	GAN	Conditional GAN-based network for generating realistic deblurred images	Uniform and non-uniform motion blur images with less blurring can be recovered	Neglecting the nonlinearity characteristics of dynamic scenes blur, the network sensory field is small and homogeneous
DeblurGAN-V2 [83]	ICCV 2019	GAN	Use feature pyramid networks and extensive backbone networks for better accuracy	Improved image restoration efficiency and enhanced real-time performance	Single network structure, which tends to lead to saturation of the network model
DBGAN [86]	CVPR 2020	GAN	Better deblurring by combining learning to generate blurred images and deblurring images	Synthetic blurred images more accurately mimic real blur for better deblurring	Network training is complex
CycleGAN [89]	ICCV 2021	GAN	Blind motion deblurring based on multi-adversarial mechanism for iterative generation of high-resolution images	Add multi-scale edge constraint function to enhance network deblurring and detail preservation capability	Presence of large color differences, severe artifacts and model redundancy
FCL-GAN [93]	MM 2022	GAN	Constraining Lightweight Network CycleGAN Driven Tasks by Frequency Domain Contrast Losses	Better deblurring of images in a lightweight and real-time manner	Deblurring effect does not reach the supervised model SOTA level
Ghost-DeblurGAN [94]	IROS 2022	GAN	Introducing GhostNet for designing lightweight deblurring networks	Suitable for real-time image deblurring, small model size, fast inference time	Deblurring effect fails to reach SOTA level
Uformer [99]	CVPR 2021	Transformer	Building hierarchical codec networks with the Transformer module	Ability to capture local and global dependencies	Self-attentive layers can only be applied to a limited depth

Table 2. A review of deep learning based deblurring methods, including publication information, overview, advantages and limitations.

Methods	Pub.	Category	Overview	Advantages	Limitations
Restormer [103]	CVPR 2022	Transformer	Codecs for learning multi-scale local-global representations of high-resolution images	Ability to model global connectivity with high computational efficiency	Image recovery does not fully utilize spatial information
Stripformer [102]	ECCV 2022	Transformer	Re-weighting image features horizontally and vertically to capture blurred features in different directions	Low memory footprint and computational cost, does not rely on large amounts of training data	Scale dot products Note that complex matrix multiplication is usually required
FFTformer [104]	CVPR 2023	Transformer	Combining a self-attentive solver with a feed-forward neural network based on discriminative frequency domain to remove blur	Lower space and time complexity and more effective and efficient in image deblurring	May not generalize well to different types of images and blurs
BiT [105]	CVPR 2023	Transformer	Introducing Double-Ended Temporal Supervision and Temporal Symmetry Integration Strategies to Generate Effective Time-Varying Motion Rendering Features	Capable of effectively handling blurring at different scales and fusing information from neighboring frames	Limited discrete supervision does not respond well to different realities
Sharpformer [111]	TIP 2023	Transformer	Adaptive handling of non-uniform blurring with dynamic convolutional blocks by fully utilizing global-local features	Able to consistently improve the quality of deblurring due to CNN-based deblurring methods alone	Higher computational complexity

Table 3. Subjective evaluation scale.

Score ↑	Quality scale	Relative quality	Absolute quality
5	There is no sign of the image quality deteriorating.	The best.	Beyond compare
4	The image quality is poor, but it is still viewable.	Better than the average level.	Nice
3	The image quality is poor, slightly hampers viewing.	The average level.	Commonly
2	Hindrance to watching.	Below average in favorability.	Bad
1	Very serious obstruction of viewing.	The worst	Very bad

3.2. Evaluation Metrics

Image quality assessment (IQA) is an important method to evaluate the effectiveness of the model. Current image quality evaluation methods can be divided into subjective and objective evaluation indexes.

3.2.1. Subjective Evaluation

Subjective evaluation relies on human judgment and is often the most intuitive method for assessing image quality. One representative measure is the Mean Opinion Score (MOS) [131]. Subjective evaluation scales primarily include absolute and relative scales. As shown in Table 3, individuals rate image quality within the range of 1-5. However, when different deblurring methods produce similar results, subjective evaluation often struggles to differentiate subtle differences. This susceptibility to individual biases and external environmental factors during assessment can lead to varying subjective evaluation results among different observers. Therefore, subjective evaluation is generally used as a supplementary assessment method in image quality evaluation and cannot entirely determine the final image quality assessment outcome. As a result, for image deblurring, most existing methods rely on objective evaluation metrics for assessment.

3.2.2. Objective Evaluation

Objective assessment primarily involves quantitatively analyzing and evaluating deblurred images through the construction of mathematical models [137–139]. Objective assessment enables the unified measurement of various deblurring methods through precise data calculations, offering advantages of fairness, objectivity, and efficiency. Among these evaluation methods, Mean Squared Error (MSE), Peak Signal-to-Noise Ratio (PSNR), and Structural Similarity Index (SSIM) stand as the most commonly employed metrics in image restoration tasks.

Mean Square Error (MSE). MSE is the average of the squared absolute errors between the restored image and the ground-truth sharp image. The closer the MSE is to zero, the smaller the difference between the restored image and the ground truth image, indicating a more realistic restoration [138].

$$\text{MSE}(\mathbf{I}, \mathbf{S}) = \frac{1}{K} \sum_{k=0}^{K-1} (\mathbf{I}_k - \mathbf{S}_k)^2, \quad (2)$$

where \mathbf{I} and \mathbf{S} represent the reconstructed image and the real sharp image, respectively. K denotes all pixels in the image.

Peak Signal Noise Ratio (PSNR). PSNR [140] is a commonly used metric to assess the effectiveness of image deblurring. It measures the accuracy of image deblurring by comparing the MSE between the deblurred and sharp images. However, PSNR only focuses on differences at the pixel level. In image deblurring assessment, it's typical to combine other metrics to comprehensively evaluate image quality. PSNR is defined as:

$$\text{PSNR}(\mathbf{I}, \mathbf{S}) = 10 \log_{10} \left(\frac{(2^n - 1)^2}{\text{MSE}(\mathbf{I}, \mathbf{S})} \right), \quad (3)$$

Table 4. Performance comparison of state-of-the-art methods on four commonly used image deblurring datasets: GoPro, HIDE, RealBlur-J, and RealBlur-R. In **red** are depicted the overall best results among all methods, while in **bold** are showcased the best results within each respective category.

Methods	Category	GoPro [61]		HIDE [113]		RealBlur-J [115]		Realblur-R [115]	
		PSNR	SSIM	PSNR	SSIM	PSNR	SSIM	PSNR	SSIM
DeepDeblur [61]	CNN	29.08	0.914	25.73	0.874	27.87	0.834	32.51	0.841
DMPHN [67]	CNN	31.20	0.940	29.09	0.924	28.42	0.860	35.70	0.948
SDWNet [126]	CNN	31.26	0.966	28.99	0.957	28.61	0.867	35.85	0.948
MSCAN [125]	CNN	31.24	0.945	29.63	0.920	-	-	-	-
PSS-NSC [123]	CNN	31.58	0.948	-	-	-	-	-	-
MIMOU-Net+ [66]	CNN	32.45	0.957	29.99	0.930	27.63	0.837	35.54	0.947
MPRNet [70]	CNN	32.66	0.959	30.96	0.939	28.70	0.873	35.99	0.952
HINet [128]	CNN	32.77	0.959	-	-	-	-	-	-
BANet [129]	CNN	32.54	0.957	30.16	0.930	-	-	-	-
SAPHNet [68]	CNN	32.02	0.953	29.98	0.930	-	-	-	-
MSSNet [127]	CNN	33.01	0.961	30.79	0.939	28.79	0.879	35.93	0.953
LaKDNet [132]	CNN	33.35	0.964	31.21	0.943	28.78	0.878	35.91	0.954
SRN [63]	RNN	30.26	0.934	28.36	0.915	28.56	0.867	35.66	0.947
MT-RNN [71]	RNN	31.15	0.945	29.15	0.918	28.44	0.862	35.79	0.951
ESTRNN [133]	RNN	31.07	0.902	-	-	-	-	-	-
IFI-RNN [134]	RNN	29.97	0.895	-	-	-	-	-	-
RNN-MBP [135]	RNN	33.32	0.963	-	-	-	-	-	-
DeblurGAN [79]	GAN	28.70	0.858	24.51	0.871	27.97	0.834	33.79	0.903
DeblurGAN-V2 [83]	GAN	29.55	0.934	26.61	0.875	28.70	0.866	35.26	0.944
DBGAN [86]	GAN	31.10	0.942	28.94	0.915	24.93	0.745	33.78	0.909
CycleGAN [89]	GAN	22.54	0.720	21.81	0.690	19.79	0.633	12.38	0.242
FCL-GAN [93]	GAN	24.84	0.771	23.43	0.732	25.35	0.736	28.37	0.663
Ghost-DeblurGAN [94]	GAN	28.75	0.919	-	-	-	-	-	-
CTMS [40]	Transformer	32.73	0.959	31.05	0.940	27.18	0.883	-	-
Uformer [99]	Transformer	32.97	0.967	30.83	0.952	29.06	0.884	36.22	0.957
Restormer [103]	Transformer	32.92	0.961	31.22	0.942	28.96	0.879	36.19	0.957
Stripformer [102]	Transformer	33.08	0.962	31.03	0.940	-	-	-	-
Stoformer [136]	Transformer	33.24	0.964	30.99	0.941	-	-	-	-
FFTformer [104]	Transformer	34.21	0.969	31.62	0.945	-	-	-	-
Sharpformer [111]	Transformer	33.10	0.963	-	-	-	-	-	-

where n is the number of digits where the image is stored. The larger the PSNR value is, the closer the recovered image is to the original image, the better the image recovery is.

Structural Similarity Index Measure(SSIM). SSIM [139] is one of the commonly used metrics in image quality assessment. In the task of image deblurring, it evaluates the similarity between the deblurred image and the ground-truth sharp image by comparing their structural information. SSIM primarily assesses image similarity based on three characteristics: luminance, contrast, and structure. It doesn't just focus on pixel differences but also considers features like image structure and texture. Compared to PSNR, SSIM aligns better with human visual perception. The calculation formula is as follows:

$$\text{SSIM}(\mathbf{I}, \mathbf{S}) = [l(\mathbf{I}, \mathbf{S})]^\alpha \cdot [c(\mathbf{I}, \mathbf{S})]^\beta \cdot [s(\mathbf{I}, \mathbf{S})]^\gamma, \quad (4)$$

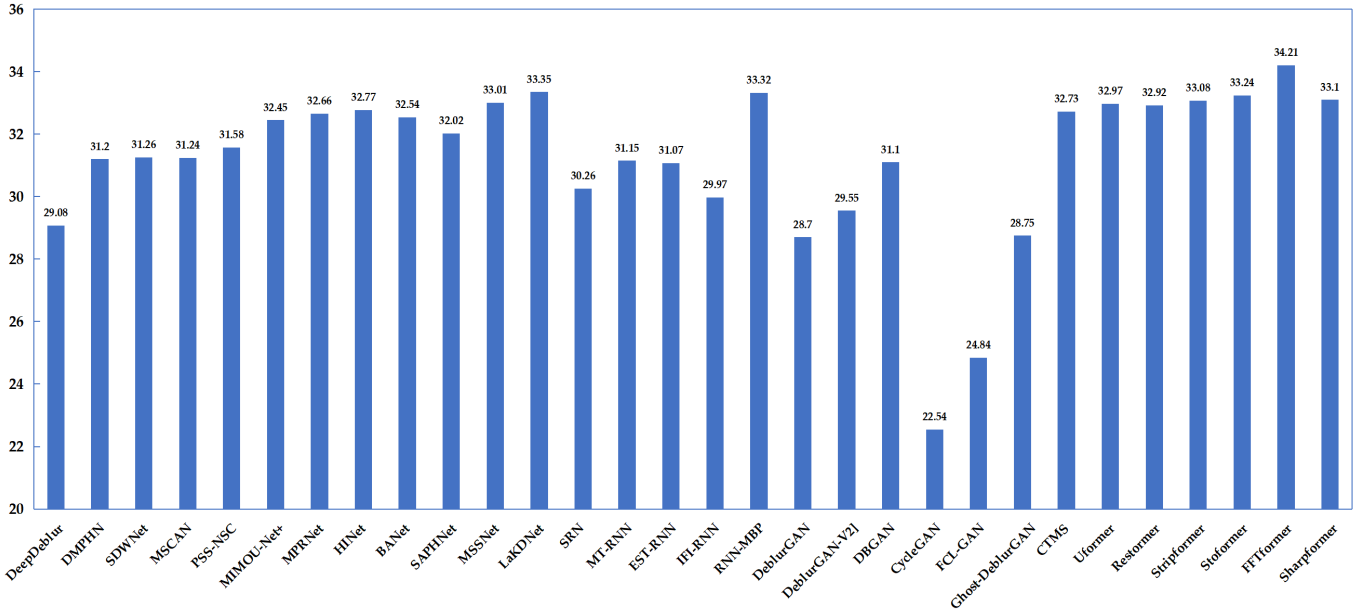


Figure 11. Performance comparison (PSNR, %) of SOTA methods on the GoPro dataset.

Table 5. Speed and Parameters of representative SOTA methods.

Method	Category	Param. (M)	Time (s)	PSNR (%)
DMPHN [67]	CNN	21.7	0.21	31.20
MIMOU-Net+ [66]	CNN	16.1	0.02	32.45
MPRNet [70]	CNN	23.0	0.09	32.66
SRN [63]	RNN	6.8	0.07	30.26
DeblurGAN-V2 [83]	GAN	60.9	0.04	29.55
Restormer [103]	Transformer	26.1	0.08	32.92
Uformer [99]	Transformer	50.9	0.07	32.97
Stripformer [102]	Transformer	19.7	0.04	33.08
FFTformer [104]	Transformer	16.6	0.13	34.21

where $l(\mathbf{I}, \mathbf{S})$ represents the brightness comparison of the image, $c(\mathbf{I}, \mathbf{S})$ represents the contrast comparison of the image, $s(\mathbf{I}, \mathbf{S})$ represents the structural comparison of the image. In engineering, often make $\alpha = \beta = \gamma = 1$. In Eq. (4),

$$l(\mathbf{I}, \mathbf{S}) = \frac{2\mu_I\mu_S + C_1}{\mu_I^2 + \mu_S^2 + C_1}, \quad c(\mathbf{I}, \mathbf{S}) = \frac{2\sigma_I\sigma_S + C_2}{\sigma_I^2 + \sigma_S^2 + C_2}, \quad s(\mathbf{I}, \mathbf{S}) = \frac{\sigma_{IS} + C_3}{\sigma_I\sigma_S + C_3}, \quad (5)$$

where μ_I , σ_I and μ_S , σ_S represent the mean, standard deviation of the images \mathbf{I} and \mathbf{S} , respectively. $\sigma_{IS} = \frac{1}{K} \sum_{k=0}^{K-1} (\mathbf{I}_k - \mu_I)(\mathbf{S}_k - \mu_S)$ indicates the covariance of the reconstructed image \mathbf{I} and the real sharp image \mathbf{S} . C is a constant to avoid the denominator 0 causing system errors. Both C_1 , C_2 and C_3 are constants, with values ranging from $[-1, 1]$. A higher SSIM value indicates a greater similarity between the restored image and the original clear image, signifying a better restoration outcome.

4. Comparison with State-of-the-Art Methods

4.1. Quantitative Comparison.

Quantitative comparisons were conducted among 30 blind motion deblurring methods across four datasets, encompassing 12 CNN-based, 5 RNN-based, 6 GAN-based, and 7 Transformer-based approaches. From Table 4, it is evident that Transformer-based methods exhibit competitive performance across the majority of datasets. This can be attributed to the self-attention mechanism in Transformers, which adeptly captures remote dependencies between local and global image sequences, enhancing the model's ability to recover details

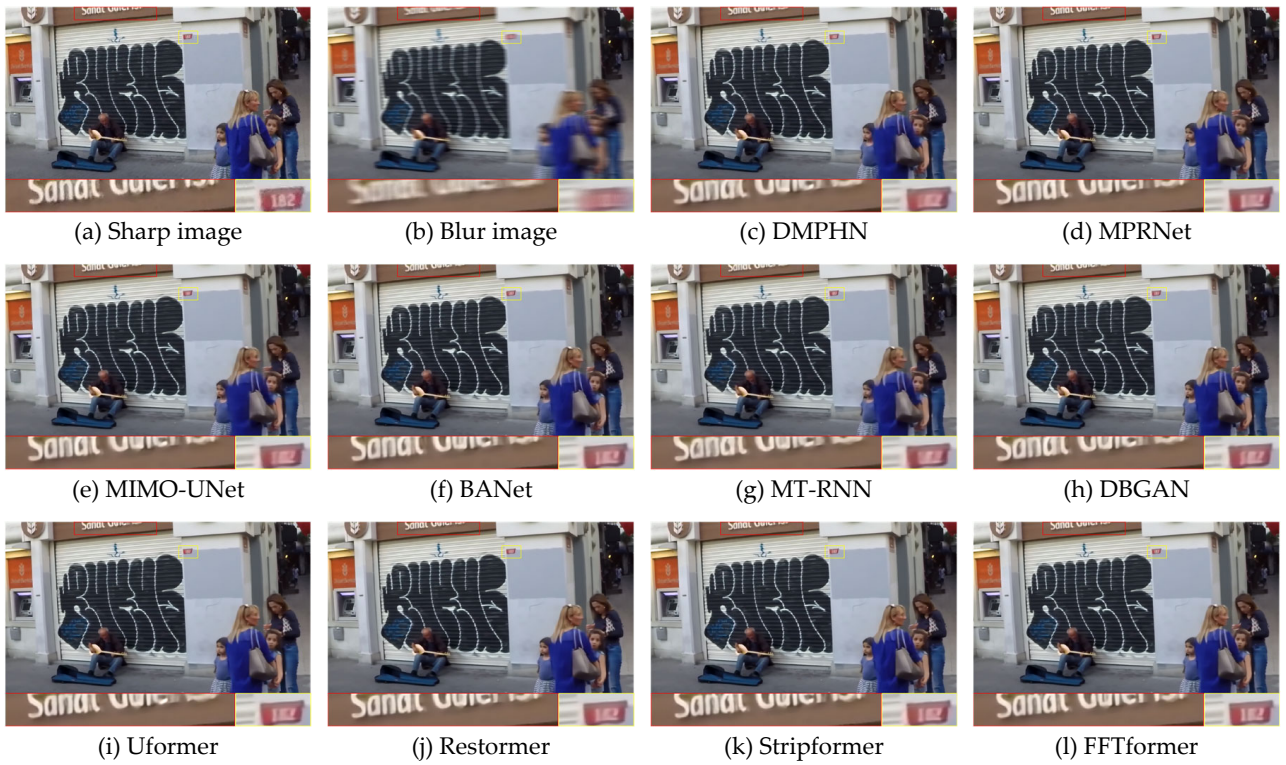


Figure 12. Comparison of background deblurring results on the GoPro dataset.

from blurred images. As depicted in Table 4, minimal performance disparities were observed between CNN and RNN methods on the GoPro dataset, both achieving over 33% PSNR and 0.96 SSIM. This similarity can be attributed partly to their analogous structures and the relatively simple motion blur in the synthetic nature of the GoPro dataset. Figure 11 illustrates that FFTformer achieved the highest PSNR score at 34.21%. Conversely, as indicated in Figure 11, the performance of GAN-based methods was inferior to other types due primarily to challenges related to training difficulties and convergence issues within GAN models, resulting in suboptimal deblurring restoration effects.

In addition, Table 5 presents a comparative analysis of various methods, balancing parameter count and operational speed. It is evident from Table 5 that RNN-based methods exhibit the smallest parameter count, CNN-based methods demonstrate the fastest operational speed, while Transformer-based methods yield the best performance. This insight further guides us toward integrating the strengths of different methodological types in subsequent research endeavors, aiming to achieve high-performance, real-time blind motion deblurring methods.

4.2. Qualitative Comparison.

As shown in Table 2, this review summarizes over 30 state-of-the-art blind motion deblurring methods based on deep learning. It includes publication details, summaries, advantages, and limitations. Among these, 22 were published in top-tier computer vision conferences such as CVPR, and ICCV, while 8 were featured in leading image processing journals like TIP, and TCSVT, among others.

To visually compare the deblurring performance of different algorithms, we conducted a qualitative assessment of selected algorithmic performance on the GoPro dataset. Figure 12 and Figure 13 illustrate the deblurring effects of various methods on backgrounds and human subjects, respectively. DBGAN and Uformer depict the deblurring results published by the original authors, while the remaining deblurred results were reproduced by us. The experiments were conducted on a Windows 10 system using Python 3.8 and Torch 2.0.0. As depicted in Figure 12 and Figure 13, the deep learning-based blind image

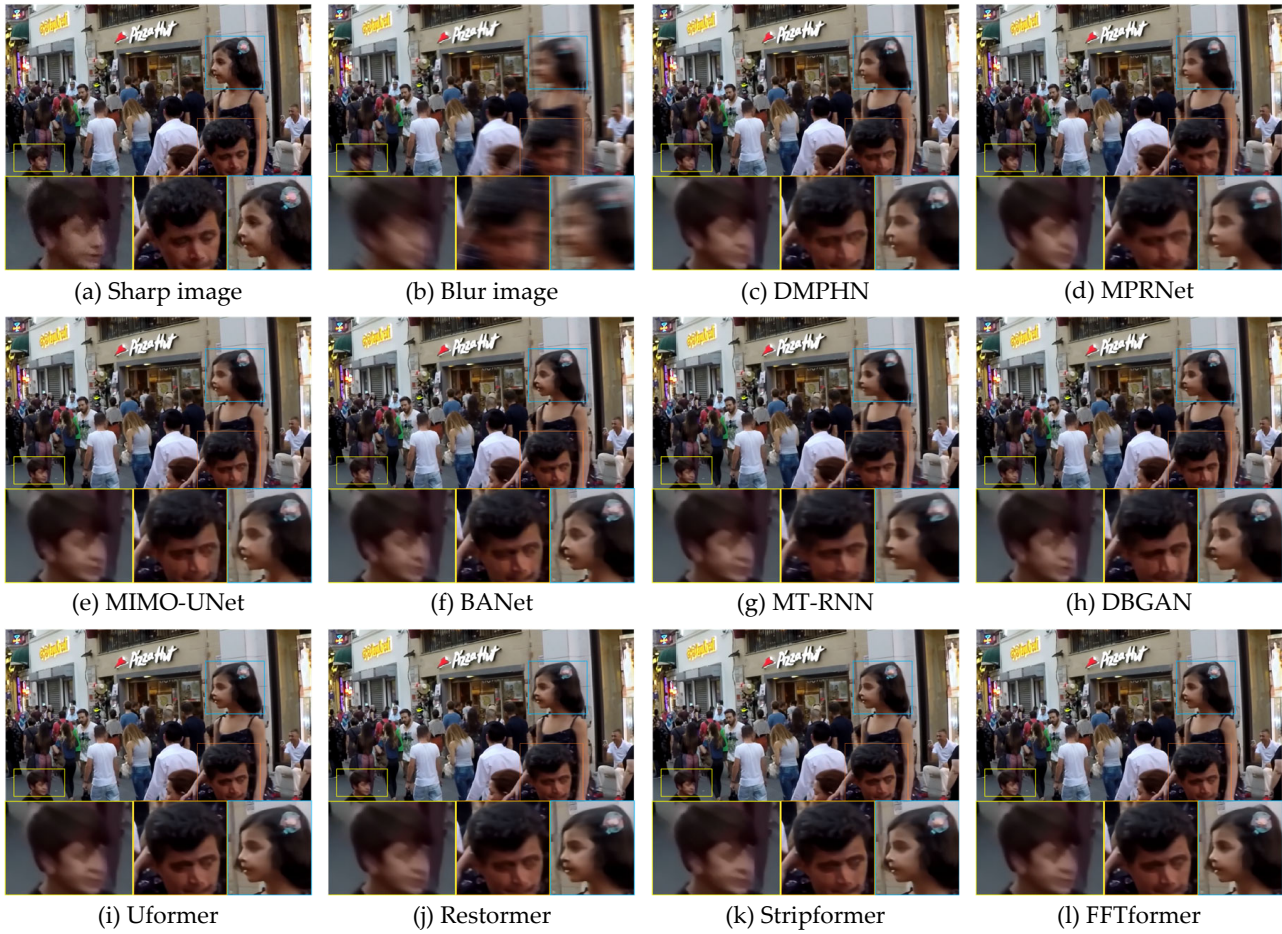


Figure 13. Comparison of human deblurring results on the GoPro dataset.

deblurring methods tested exhibit effective image restoration. While some differences persist compared to the original clear images, visually, they do not significantly impact the image information. Combining the insights from Table 4 and Figure 13, it becomes apparent that Transformer-based models not only outperform other methods in evaluation metrics such as PSNR and SSIM but also demonstrate superior restoration of image details throughout the image recovery process.

5. Current Challenges and Future Prospects

5.1. Challenges of Blind Motion Deblurring and Major Concerns

The paper provides an overview of image deblurring algorithms based on deep learning, encompassing methods such as CNN-based, RNN-based, GAN-based, and Transformer-based image deblurring techniques. These methods are analyzed, compared, and summarized, and their performance is contrasted.

Despite the progress made in image deblurring algorithms concerning restoration effects, challenges persist due to the complexity of real-world blur scenarios. The challenges of blind motion deblurring and major concerns are as follows:

(1) **Generalization Ability of Model:** As shown in Table 6, the model trained on synthetic datasets exhibits poor generalization on real datasets. Compared with the training on the real datasets, the overall performance of the methods trained on the synthetic dataset decreases by about 3%, and the SSIM value will decrease by at least 0.02 in Table 6. Enhancing the generalization of model is a question that needs to be addressed.

(2) **Data Requirements and Diversity:** Most deep learning-based image deblurring algorithms rely on training with clear-blurred image pairs. The types of motion blur are diverse. Handling different types and intensities of motion blur requires a large amount of

Table 6. Comparison of generalization performance on real motion blur datasets.

Methods	Trained on GoPro				Trained on Realblur			
	RealBlur-J		Realblur-R		RealBlur-J		Realblur-R	
	PSNR	SSIM	PSNR	SSIM	PSNR	SSIM	PSNR	SSIM
SRN [63]	28.56	0.867	35.66	0.947	31.38	0.909	38.65	0.965
SDWNet [126]	28.61	0.867	35.85	0.948	30.73	0.896	38.21	0.963
DeblurGAN-V2 [83]	28.70	0.866	35.26	0.944	29.69	0.870	36.44	0.935
MPRNet [70]	28.70	0.873	35.99	0.952	31.76	0.922	39.31	0.972
MSSNet [127]	28.79	0.879	35.93	0.953	32.10	0.928	39.76	0.972
LaKDNNet [132]	28.78	0.878	35.91	0.954	32.33	0.929	39.91	0.974
MAXIM-3S [141]	28.83	0.875	35.78	0.947	32.84	0.935	39.45	0.962
DeepRFT+ [142]	28.97	0.884	36.06	0.954	32.19	0.931	39.84	0.972

diverse data. Collecting and labeling this data might be a challenge, especially considering the types of blur, lighting conditions, and scene variations.

(3) Balancing Model Performance and Light-weight Models: Increasing model depth and parameters can enhance fitting data and improve image restoration quality. However, this can lead to larger network sizes, longer inference times, and higher computational complexity. Finding a balance between model performance and model light-weighting for practical applications is an essential area for exploration.

(4) Deblurring Methods for High-Level Visual Tasks: Blurred images hinder several advanced computer vision tasks, yet many existing deblurring methods aim solely at recovering high-quality images without considering aiding higher-level tasks such as object detection [143–145] or image segmentation [146,147]. Research focusing on effectively extracting relevant features for high-level visual problems to enhance image deblurring solutions is a promising direction.

5.2. Future Prospects

(1) More comprehensive datasets: Most deep learning-based image deblurring algorithms rely on training data comprising blurred images. Constructing a more comprehensive dataset that encompasses a broader range of application scenarios can empower models to better handle various real-world situations, such as motion blur, low-light conditions, and lens shake. However, building such a comprehensive dataset poses challenges. Collecting and labeling various types of blurry images may require substantial time and resources. Moreover, ensuring the quality and diversity of the dataset is crucial, as low-quality or imbalanced data could adversely affect model training.

(2) More innovative network structure: Considering the complexity of image deblurring and the practical demands of applications, it's essential to innovate and improve the deblurring network architectures. Combining the latest advancements in deep learning, these architectures may better capture complex blur patterns within images. This enhancement could enable them to address various types and intensities of blur, allowing models to perform exceptionally well across a broader range of scenarios.

(3) More objective evaluation indicators: Current evaluation metrics may fail to capture all subtle variations in the image deblurring process. Hence, more objective and comprehensive metrics are crucial for assessing algorithm effectiveness and performance enhancements. Considering multiple aspects such as clarity, detail retention, noise, contrast, etc., constructing comprehensive evaluation metrics would better assess the effectiveness of image deblurring. Introducing evaluation metrics aligned with human visual perception, beyond pixel-level metrics, considering the human perception of details, contrast, color, etc., might better reflect the performance of image deblurring techniques.

(4) Few-shot learning: Traditional deep learning models often require extensive labeled data for training, which might be challenging to obtain, especially high-quality labeled clear

images. Few-shot learning [148–150] help models rapidly learn and adapt to new tasks from a limited amount of labeled data, reducing dependence on extensive labeled datasets. This approach addresses challenges related to acquiring and labeling data, potentially widening the application of image deblurring techniques across real-world scenarios.

(5) Applications of diffusion: The Diffusion model is a generative model that has garnered significant attention in recent years, demonstrating immense potential in the realm of image editing and enhancement. In the field of image deblurring, the Diffusion model has also found applications [151,152]. Its flexibility allows it to handle various types of noise and transformations, suggesting its capability to potentially address complex image blurring. In the future, with a deeper understanding of the Diffusion model and the development of related techniques, it is poised to become a significant tool in the domain of image deblurring, promising more satisfying results and improvements.

(6) Unsupervised Deblurring Methods: Real-world blurry images often lack corresponding clear counterparts. Employing unsupervised methods [153] could render algorithms robust against real-world blurry scenarios, operating without extensive training data.

6. Conclusions

The current research and developments indicate significant progress in enhancing image quality and clarity through deep learning technologies. This paper reviews recent advancements in deep learning-based image deblurring algorithms, providing a comprehensive classification and analysis. It elaborates on existing image deblurring algorithms from four perspectives: CNN, RNN, GAN, and Transformer. Additionally, it conducts comparative analyses of representative algorithms, summarizing their strengths and limitations. Finally, the paper outlines future research directions in image deblurring algorithms. However, it is acknowledged that addressing more complex blurs in real-world scenarios remains a challenge. The quality of data and the accuracy of labels are crucial for training deep learning models, necessitating large-scale, high-quality datasets to support model training and optimization. In the future, there is an anticipation to further optimize deep learning models to enhance their speed and efficiency, expanding the application of these techniques in fields such as video processing, surveillance, and autonomous driving.

Author Contributions: Methodology, Y.X.; Supervision, Z.L. and Y.X.; Writing—Original Draft, Y.X., H.Z. and C.L.; Writing—Review and Editing, Y.X., H.Z. and F.S.; Visualization, Y.X., F.S., C.L. and H.Z.; All authors have read and agreed to the published version of the manuscript.

Funding: This research received no external funding.

Data Availability Statement: Not applicable.

Conflicts of Interest: The authors declare no conflict of interest.

References

1. Burdziakowski, P. A Novel Method for the Deblurring of Photogrammetric Images Using Conditional Generative Adversarial Networks. *Remote Sensing* **2020**, *12*, 2586.
2. Peng, Y.; Tang, Z.; Zhao, G.; Cao, G.; Wu, C. Motion blur removal for UAV-based wind turbine blade images using synthetic datasets. *Remote Sensing* **2021**, *14*, 87.
3. Rengarajan, V.; Rajagopalan, A.N.; Aravind, R.; Seetharaman, G. Image registration and change detection under rolling shutter motion blur. *IEEE Transactions on Pattern Analysis and Machine Intelligence* **2016**, *39*, 1959–1972.
4. Li, C.; Zhou, H.; Liu, Y.; Yang, C.; Xie, Y.; Li, Z.; Zhu, L. Detection-friendly dehazing: object detection in real-world hazy scenes. *IEEE Transactions on Pattern Analysis and Machine Intelligence* **2023**, *45*, 8284–8295.
5. Rajagopalan, A.; et al. Improving Robustness of Semantic Segmentation to Motion-Blur Using Class-Centric Augmentation. In Proceedings of the Proceedings of the IEEE/CVF Conference on Computer Vision and Pattern Recognition, 2023, pp. 10470–10479.
6. Zhou, H.; Tian, C.; Zhang, Z.; Li, C.; Ding, Y.; Xie, Y.; Li, Z. Position-Aware Relation Learning for RGB-Thermal Salient Object Detection. *IEEE Transactions on Image Processing* **2023**, *32*, 2593–2607.

7. Zhang, W.; Bergholm, F. Multi-scale blur estimation and edge type classification for scene analysis. *International Journal of Computer Vision* **1997**, *24*, 219–250.
8. Zhou, H.; Tian, C.; Zhang, Z.; Li, C.; Xie, Y.; Li, Z. PixelGame: Infrared small target segmentation as a Nash equilibrium. *IEEE Journal of Selected Topics in Applied Earth Observations and Remote Sensing* **2022**, *15*, 8010–8024.
9. Chen, J.; Yu, H.; Xu, G.; Zhang, J.; Liang, B.; Yang, D. Airborne SAR Autofocus Based on Blurry Imagery Classification. *Remote Sensing* **2021**, *13*, 3872.
10. Bai, Y.; Jia, H.; Jiang, M.; Liu, X.; Xie, X.; Gao, W. Single-image blind deblurring using multi-scale latent structure prior. *IEEE Transactions on Circuits and Systems for Video Technology* **2019**, *30*, 2033–2045.
11. Zhang, Z.; Zheng, L.; Piao, Y.; Tao, S.; Xu, W.; Gao, T.; Wu, X. Blind remote sensing image deblurring using local binary pattern prior. *Remote Sensing* **2022**, *14*, 1276.
12. Arjomand Bigdeli, S.; Zwicker, M.; Favaro, P.; Jin, M. Deep mean-shift priors for image restoration. *Advances in Neural Information Processing Systems* **2017**, *30*.
13. Sun, L.; Cho, S.; Wang, J.; Hays, J. Good image priors for non-blind deconvolution: generic vs. specific. In Proceedings of the Computer Vision–ECCV 2014: 13th European Conference, Zurich, Switzerland, September 6–12, 2014, Proceedings, Part IV 13. Springer, 2014, pp. 231–246.
14. Zhang, K.; Zuo, W.; Gu, S.; Zhang, L. Learning deep CNN denoiser prior for image restoration. In Proceedings of the Proceedings of the IEEE Conference on Computer Vision and Pattern Recognition, 2017, pp. 3929–3938.
15. Pan, J.; Sun, D.; Pfister, H.; Yang, M.H. Blind image deblurring using dark channel prior. In Proceedings of the Proceedings of the IEEE Conference on Computer Vision and Pattern Recognition, 2016, pp. 1628–1636.
16. Chen, L.; Fang, F.; Wang, T.; Zhang, G. Blind image deblurring with local maximum gradient prior. In Proceedings of the Proceedings of the IEEE/CVF Conference on Computer Vision and Pattern Recognition, 2019, pp. 1742–1750.
17. Hu, Z.; Cho, S.; Wang, J.; Yang, M.H. Deblurring low-light images with light streaks. In Proceedings of the Proceedings of the IEEE Conference on Computer Vision and Pattern Recognition, 2014, pp. 3382–3389.
18. Yan, Y.; Ren, W.; Guo, Y.; Wang, R.; Cao, X. Image deblurring via extreme channels prior. In Proceedings of the Proceedings of the IEEE Conference on Computer Vision and Pattern Recognition, 2017, pp. 4003–4011.
19. Liu, J.; Yan, M.; Zeng, T. Surface-aware blind image deblurring. *IEEE Transactions on Pattern Analysis and Machine Intelligence* **2019**, *43*, 1041–1055.
20. Zhai, L.; Wang, Y.; Cui, S.; Zhou, Y. A Comprehensive Review of Deep Learning-Based Real-World Image Restoration. *IEEE Access* **2023**.
21. Zhang, K.; Ren, W.; Luo, W.; Lai, W.S.; Stenger, B.; Yang, M.H.; Li, H. Deep image deblurring: A survey. *International Journal of Computer Vision* **2022**, *130*, 2103–2130.
22. Levin, A. Blind motion deblurring using image statistics. *Advances in Neural Information Processing Systems* **2006**, *19*.
23. Yang, L.; Ji, H. A variational EM framework with adaptive edge selection for blind motion deblurring. In Proceedings of the Proceedings of the IEEE/CVF Conference on Computer Vision and Pattern Recognition, 2019, pp. 10167–10176.
24. Fergus, R.; Singh, B.; Hertzmann, A.; Roweis, S.T.; Freeman, W.T. Removing camera shake from a single photograph. In *Acm Siggraph 2006 Papers*; 2006; pp. 787–794.
25. Krishnan, D.; Tay, T.; Fergus, R. Blind deconvolution using a normalized sparsity measure. In Proceedings of the Proceedings of the IEEE/CVF Conference on Computer Vision and Pattern Recognition. IEEE, 2011, pp. 233–240.
26. Xu, L.; Zheng, S.; Jia, J. Unnatural l0 sparse representation for natural image deblurring. In Proceedings of the Proceedings of the IEEE Conference on Computer Vision and Pattern Recognition, 2013, pp. 1107–1114.
27. Levin, A.; Weiss, Y.; Durand, F.; Freeman, W.T. Efficient marginal likelihood optimization in blind deconvolution. In Proceedings of the Proceedings of the IEEE/CVF Conference on Computer Vision and Pattern Recognition. IEEE, 2011, pp. 2657–2664.
28. Sun, L.; Cho, S.; Wang, J.; Hays, J. Edge-based blur kernel estimation using patch priors. In Proceedings of the IEEE International Conference on Computational Photography (ICCP). IEEE, 2013, pp. 1–8.
29. Guo, Y.; Ma, H. Image blind deblurring using an adaptive patch prior. *Tsinghua Science and Technology* **2018**, *24*, 238–248.
30. Tang, Y.; Xue, Y.; Chen, Y.; Zhou, L. Blind deblurring with sparse representation via external patch priors. *Digital Signal Processing* **2018**, *78*, 322–331.
31. Pan, J.; Sun, D.; Pfister, H.; Yang, M.H. Deblurring images via dark channel prior. *IEEE Transactions on Pattern Analysis and Machine Intelligence* **2017**, *40*, 2315–2328.
32. Ge, X.; Tan, J.; Zhang, L. Blind image deblurring using a non-linear channel prior based on dark and bright channels. *IEEE Transactions on Image Processing* **2021**, *30*, 6970–6984.
33. Cai, J.; Zuo, W.; Zhang, L. Dark and bright channel prior embedded network for dynamic scene deblurring. *IEEE Transactions on Image Processing* **2020**, *29*, 6885–6897.
34. Levin, A.; Weiss, Y.; Durand, F.; Freeman, W.T. Understanding and evaluating blind deconvolution algorithms. In Proceedings of the 2009 IEEE Conference on Computer Vision and Pattern Recognition. IEEE, 2009, pp. 1964–1971.
35. Pan, J.; Hu, Z.; Su, Z.; Yang, M.H. Deblurring text images via L0-regularized intensity and gradient prior. In Proceedings of the Proceedings of the IEEE Conference on Computer Vision and Pattern Recognition, 2014, pp. 2901–2908.
36. Shao, W.Z.; Lin, Y.Z.; Liu, Y.Y.; Wang, L.Q.; Ge, Q.; Bao, B.K.; Li, H.B. Gradient-based discriminative modeling for blind image deblurring. *Neurocomputing* **2020**, *413*, 305–327.

37. Zhang, K.; Gao, X.; Tao, D.; Li, X. Single image super-resolution with non-local means and steering kernel regression. *IEEE Transactions on Image Processing* **2012**, *21*, 4544–4556.
38. Zhou, H.; Tian, C.; Zhang, Z.; Li, C.; Xie, Y.; Li, Z. Frequency-aware Feature Aggregation Network with Dual-task Consistency for RGB-T Salient Object Detection. *Pattern Recognition* **2024**, *146*, 110043.
39. Gu, C.; Lu, X.; He, Y.; Zhang, C. Blur removal via blurred-noisy image pair. *IEEE Transactions on Image Processing* **2020**, *30*, 345–359.
40. Zhao, Q.; Yang, H.; Zhou, D.; Cao, J. Rethinking Image Deblurring via CNN-Transformer Multiscale Hybrid Architecture. *IEEE Transactions on Instrumentation and Measurement* **2022**, *72*, 1–15.
41. Purohit, K.; Suin, M.; Rajagopalan, A.; Boddeti, V.N. Spatially-adaptive image restoration using distortion-guided networks. In Proceedings of the Proceedings of the IEEE/CVF International Conference on Computer Vision, 2021, pp. 2309–2319.
42. Chen, L.; Chu, X.; Zhang, X.; Sun, J. Simple baselines for image restoration. In Proceedings of the European Conference on Computer Vision. Springer, 2022, pp. 17–33.
43. Yang, D.; Yamac, M. Motion aware double attention network for dynamic scene deblurring. In Proceedings of the Proceedings of the IEEE/CVF Conference on Computer Vision and Pattern Recognition, 2022, pp. 1113–1123.
44. Nimisha, T.M.; Kumar Singh, A.; Rajagopalan, A.N. Blur-invariant deep learning for blind-deblurring. In Proceedings of the Proceedings of the IEEE International Conference on Computer Vision, 2017, pp. 4752–4760.
45. Mao, X.; Shen, C.; Yang, Y.B. Image restoration using very deep convolutional encoder-decoder networks with symmetric skip connections. *Advances in Neural Information Processing Systems* **2016**, *29*.
46. Goodfellow, I.; Pouget-Abadie, J.; Mirza, M.; Xu, B.; Warde-Farley, D.; Ozair, S.; Courville, A.; Bengio, Y. Generative adversarial nets. *Advances in Neural Information Processing Systems* **2014**, *27*.
47. Wang, X.; Sun, L.; Chehri, A.; Song, Y. A Review of GAN-Based Super-Resolution Reconstruction for Optical Remote Sensing Images. *Remote Sensing* **2023**, *15*, 5062.
48. Zhang, J.; Pan, J.; Ren, J.; Song, Y.; Bao, L.; Lau, R.W.; Yang, M.H. Dynamic scene deblurring using spatially variant recurrent neural networks. In Proceedings of the Proceedings of the IEEE Conference on Computer Vision and Pattern Recognition, 2018, pp. 2521–2529.
49. Zhao, S.; Xing, Y.; Xu, H. WTransU-Net: Wiener deconvolution meets multi-scale transformer-based U-net for image deblurring. *Signal, Image and Video Processing* **2023**, pp. 1–9.
50. Li, J.; Tan, W.; Yan, B. Perceptual variousness motion deblurring with light global context refinement. In Proceedings of the Proceedings of the IEEE/CVF International Conference on Computer Vision, 2021, pp. 4116–4125.
51. Yuan, Y.; Su, W.; Ma, D. Efficient dynamic scene deblurring using spatially variant deconvolution network with optical flow guided training. In Proceedings of the Proceedings of the IEEE/CVF Conference on Computer Vision and Pattern Recognition, 2020, pp. 3555–3564.
52. Noroozi, M.; Chandramouli, P.; Favaro, P. Motion deblurring in the wild. In Proceedings of the Pattern Recognition: 39th German Conference, GCPR 2017, Basel, Switzerland, September 12–15, 2017, Proceedings 39. Springer, 2017, pp. 65–77.
53. Schuler, C.J.; Hirsch, M.; Harmeling, S.; Schölkopf, B. Learning to deblur. *IEEE Transactions on Pattern Analysis and Machine Intelligence* **2015**, *38*, 1439–1451.
54. Sun, J.; Cao, W.; Xu, Z.; Ponce, J. Learning a convolutional neural network for non-uniform motion blur removal. In Proceedings of the Proceedings of the IEEE Conference on Computer Vision and Pattern Recognition, 2015, pp. 769–777.
55. Cronje, J. Deep convolutional neural networks for dense non-uniform motion deblurring. In Proceedings of the 2015 International Conference on Image and Vision Computing New Zealand (IVCNZ). IEEE, 2015, pp. 1–5.
56. Chakrabarti, A. A neural approach to blind motion deblurring. In Proceedings of the Computer Vision–ECCV 2016: 14th European Conference, Amsterdam, The Netherlands, October 11–14, 2016, Proceedings, Part III 14. Springer, 2016, pp. 221–235.
57. Gong, D.; Yang, J.; Liu, L.; Zhang, Y.; Reid, I.; Shen, C.; Van Den Hengel, A.; Shi, Q. From motion blur to motion flow: A deep learning solution for removing heterogeneous motion blur. In Proceedings of the Proceedings of the IEEE Conference on Computer Vision and Pattern Recognition, 2017, pp. 2319–2328.
58. Xu, X.; Pan, J.; Zhang, Y.J.; Yang, M.H. Motion blur kernel estimation via deep learning. *IEEE Transactions on Image Processing* **2017**, *27*, 194–205.
59. Kaufman, A.; Fattal, R. Deblurring using analysis-synthesis networks pair. In Proceedings of the Proceedings of the IEEE/CVF Conference on Computer Vision and Pattern Recognition, 2020, pp. 5811–5820.
60. Xu, L.; Ren, J.S.; Liu, C.; Jia, J. Deep convolutional neural network for image deconvolution. *Advances in Neural Information Processing Systems* **2014**, *27*.
61. Nah, S.; Hyun Kim, T.; Mu Lee, K. Deep multi-scale convolutional neural network for dynamic scene deblurring. In Proceedings of the Proceedings of the IEEE Conference on Computer Vision and Pattern Recognition, 2017, pp. 3883–3891.
62. Purohit, K.; Rajagopalan, A. Region-adaptive dense network for efficient motion deblurring. In Proceedings of the Proceedings of the AAAI Conference on Artificial Intelligence, 2020, Vol. 34, pp. 11882–11889.
63. Tao, X.; Gao, H.; Shen, X.; Wang, J.; Jia, J. Scale-recurrent network for deep image deblurring. In Proceedings of the Proceedings of the IEEE Conference on Computer Vision and Pattern Recognition, 2018, pp. 8174–8182.
64. Vitoria, P.; Georgoulis, S.; Tulyakov, S.; Bochicchio, A.; Erbach, J.; Li, Y. Event-based image deblurring with dynamic motion awareness. In Proceedings of the European Conference on Computer Vision. Springer, 2022, pp. 95–112.

65. Hemanth, K.; Latha, H. Dynamic scene Image deblurring using modified scale-recurrent network. In Proceedings of the 2020 4th International Conference on Electronics, Communication and Aerospace Technology (ICECA). IEEE, 2020, pp. 966–973.
66. Cho, S.J.; Ji, S.W.; Hong, J.P.; Jung, S.W.; Ko, S.J. Rethinking coarse-to-fine approach in single image deblurring. In Proceedings of the Proceedings of the IEEE/CVF International Conference on Computer Vision, 2021, pp. 4641–4650.
67. Zhang, H.; Dai, Y.; Li, H.; Koniusz, P. Deep stacked hierarchical multi-patch network for image deblurring. In Proceedings of the Proceedings of the IEEE/CVF Conference on Computer Vision and Pattern Recognition, 2019, pp. 5978–5986.
68. Suin, M.; Purohit, K.; Rajagopalan, A. Spatially-attentive patch-hierarchical network for adaptive motion deblurring. In Proceedings of the Proceedings of the IEEE/CVF Conference on Computer Vision and Pattern Recognition, 2020, pp. 3606–3615.
69. Zhang, H.; Zhang, L.; Dai, Y.; Li, H.; Koniusz, P. Event-guided multi-patch network with self-supervision for non-uniform motion deblurring. *International Journal of Computer Vision* **2023**, *131*, 453–470.
70. Zamir, S.W.; Arora, A.; Khan, S.; Hayat, M.; Khan, F.S.; Yang, M.H.; Shao, L. Multi-stage progressive image restoration. In Proceedings of the Proceedings of the IEEE/CVF Conference on Computer Vision and Pattern Recognition, 2021, pp. 14821–14831.
71. Park, D.; Kang, D.U.; Kim, J.; Chun, S.Y. Multi-temporal recurrent neural networks for progressive non-uniform single image deblurring with incremental temporal training. In Proceedings of the European Conference on Computer Vision. Springer, 2020, pp. 327–343.
72. Zhang, X.; Yu, L.; Yang, W.; Liu, J.; Xia, G.S. Generalizing Event-Based Motion Deblurring in Real-World Scenarios. In Proceedings of the Proceedings of the IEEE/CVF International Conference on Computer Vision, 2023, pp. 10734–10744.
73. Zhang, C.; Zhang, X.; Lin, M.; Li, C.; He, C.; Yang, W.; Xia, G.S.; Yu, L. CrossZoom: Simultaneously Motion Deblurring and Event Super-Resolving. *arXiv preprint arXiv:2309.16949* **2023**.
74. Liping, L.; Jian, S.; Shiyan, G. Overview of Blind Deblurring Methods for Single Image. *Journal of Frontiers of Computer Science & Technology* **2022**, *16*.
75. Ren, W.; Zhang, J.; Pan, J.; Liu, S.; Ren, J.S.; Du, J.; Cao, X.; Yang, M.H. Deblurring dynamic scenes via spatially varying recurrent neural networks. *IEEE Transactions on Pattern Analysis and Machine Intelligence* **2021**, *44*, 3974–3987.
76. Ramakrishnan, S.; Pachori, S.; Gangopadhyay, A.; Raman, S. Deep generative filter for motion deblurring. In Proceedings of the Proceedings of the IEEE International Conference on Computer Vision workshops, 2017, pp. 2993–3000.
77. Lin, J.C.; Wei, W.L.; Liu, T.L.; Kuo, C.C.J.; Liao, M. Tell me where it is still blurry: Adversarial blurred region mining and refining. In Proceedings of the Proceedings of the 27th ACM International Conference on Multimedia, 2019, pp. 702–710.
78. Mirza, M.; Osindero, S. Conditional generative adversarial nets. *arXiv preprint arXiv:1411.1784* **2014**.
79. Kupyn, O.; Budzan, V.; Mykhailych, M.; Mishkin, D.; Matas, J. Deblurgan: Blind motion deblurring using conditional adversarial networks. In Proceedings of the Proceedings of the IEEE Conference on Computer Vision and Pattern Recognition, 2018, pp. 8183–8192.
80. Arjovsky, M.; Chintala, S.; Bottou, L. Wasserstein generative adversarial networks. In Proceedings of the International Conference on Machine Learning. PMLR, 2017, pp. 214–223.
81. Gulrajani, I.; Ahmed, F.; Arjovsky, M.; Dumoulin, V.; Courville, A.C. Improved training of wasserstein gans. *Advances in Neural Information Processing Systems* **2017**, *30*.
82. Johnson, J.; Alahi, A.; Fei-Fei, L. Perceptual losses for real-time style transfer and super-resolution. In Proceedings of the Computer Vision–ECCV 2016: 14th European Conference, Amsterdam, The Netherlands, October 11–14, 2016, Proceedings, Part II 14. Springer, 2016, pp. 694–711.
83. Kupyn, O.; Martyniuk, T.; Wu, J.; Wang, Z. Deblurgan-v2: Deblurring (orders-of-magnitude) faster and better. In Proceedings of the Proceedings of the IEEE/CVF International Conference on Computer Vision, 2019, pp. 8878–8887.
84. Peng, J.; Guan, T.; Liu, F.; Liang, J. MND-GAN: A Research on Image Deblurring Algorithm Based on Generative Adversarial Network. In Proceedings of the 2023 42nd Chinese Control Conference (CCC). IEEE, 2023, pp. 7584–7589.
85. Zheng, S.; Zhu, Z.; Cheng, J.; Guo, Y.; Zhao, Y. Edge heuristic GAN for non-uniform blind deblurring. *IEEE Signal Processing Letters* **2019**, *26*, 1546–1550.
86. Zhang, K.; Luo, W.; Zhong, Y.; Ma, L.; Stenger, B.; Liu, W.; Li, H. Deblurring by realistic blurring. In Proceedings of the Proceedings of the IEEE/CVF Conference on Computer Vision and Pattern Recognition, 2020, pp. 2737–2746.
87. Nimisha, T.M.; Sunil, K.; Rajagopalan, A. Unsupervised class-specific deblurring. In Proceedings of the Proceedings of the European Conference on Computer Vision, 2018, pp. 353–369.
88. Mescheder, L.; Geiger, A.; Nowozin, S. Which training methods for GANs do actually converge? In Proceedings of the International Conference on Machine Learning. PMLR, 2018, pp. 3481–3490.
89. Zhu, J.Y.; Park, T.; Isola, P.; Efros, A.A. Unpaired image-to-image translation using cycle-consistent adversarial networks. In Proceedings of the Proceedings of the IEEE International Conference on Computer Vision, 2017, pp. 2223–2232.
90. Wen, Y.; Chen, J.; Sheng, B.; Chen, Z.; Li, P.; Tan, P.; Lee, T.Y. Structure-aware motion deblurring using multi-adversarial optimized cyclegan. *IEEE Transactions on Image Processing* **2021**, *30*, 6142–6155.
91. Zhao, B.; Li, W.; Gong, W. Real-aware motion deblurring using multi-attention CycleGAN with contrastive guidance. *Digital Signal Processing* **2023**, *135*, 103953.
92. Lu, B.; Chen, J.C.; Chellappa, R. UID-GAN: Unsupervised image deblurring via disentangled representations. *IEEE Transactions on Biometrics, Behavior, and Identity Science* **2019**, *2*, 26–39.

93. Zhao, S.; Zhang, Z.; Hong, R.; Xu, M.; Yang, Y.; Wang, M. FCL-GAN: A lightweight and real-time baseline for unsupervised blind image deblurring. In Proceedings of the Proceedings of the 30th ACM International Conference on Multimedia, 2022, pp. 6220–6229.
94. Liu, Y.; Haridevan, A.; Schofield, H.; Shan, J. Application of Ghost-DeblurGAN to Fiducial Marker Detection. In Proceedings of the 2022 IEEE/RSJ International Conference on Intelligent Robots and Systems (IROS). IEEE, 2022, pp. 6827–6832.
95. Vaswani, A.; Shazeer, N.; Parmar, N.; Uszkoreit, J.; Jones, L.; Gomez, A.N.; Kaiser, L.; Polosukhin, I. Attention is all you need. *Advances in Neural Information Processing Systems* **2017**, *30*.
96. Liu, Z.; Lin, Y.; Cao, Y.; Hu, H.; Wei, Y.; Zhang, Z.; Lin, S.; Guo, B. Swin transformer: Hierarchical vision transformer using shifted windows. In Proceedings of the Proceedings of the IEEE/CVF International Conference on Computer Vision, 2021, pp. 10012–10022.
97. Zhou, H.; Tian, C.; Zhang, Z.; Huo, Q.; Xie, Y.; Li, Z. Multispectral fusion transformer network for RGB-thermal urban scene semantic segmentation. *IEEE Geoscience and Remote Sensing Letters* **2022**, *19*, 1–5.
98. Raghu, M.; Unterthiner, T.; Kornblith, S.; Zhang, C.; Dosovitskiy, A. Do vision transformers see like convolutional neural networks? *Advances in Neural Information Processing Systems* **2021**, *34*, 12116–12128.
99. Wang, Z.; Cun, X.; Bao, J.; Zhou, W.; Liu, J.; Li, H. Uformer: A general u-shaped transformer for image restoration. In Proceedings of the Proceedings of the IEEE/CVF Conference on Computer Vision and Pattern Recognition, 2022, pp. 17683–17693.
100. Ronneberger, O.; Fischer, P.; Brox, T. U-net: Convolutional networks for biomedical image segmentation. In Proceedings of the Medical Image Computing and Computer-Assisted Intervention–MICCAI 2015: 18th International Conference, Munich, Germany, October 5–9, 2015, Proceedings, Part III 18. Springer, 2015, pp. 234–241.
101. Ji, H.; Feng, X.; Pei, W.; Li, J.; Lu, G. U2-former: A nested u-shaped transformer for image restoration. *arXiv preprint arXiv:2112.02279* **2021**.
102. Tsai, F.J.; Peng, Y.T.; Lin, Y.Y.; Tsai, C.C.; Lin, C.W. Stripformer: Strip transformer for fast image deblurring. In Proceedings of the European Conference on Computer Vision. Springer, 2022, pp. 146–162.
103. Zamir, S.W.; Arora, A.; Khan, S.; Hayat, M.; Khan, F.S.; Yang, M.H. Restormer: Efficient transformer for high-resolution image restoration. In Proceedings of the Proceedings of the IEEE/CVF Conference on Computer Vision and Pattern Recognition, 2022, pp. 5728–5739.
104. Kong, L.; Dong, J.; Ge, J.; Li, M.; Pan, J. Efficient Frequency Domain-based Transformers for High-Quality Image Deblurring. In Proceedings of the Proceedings of the IEEE/CVF Conference on Computer Vision and Pattern Recognition, 2023, pp. 5886–5895.
105. Zhong, Z.; Cao, M.; Ji, X.; Zheng, Y.; Sato, I. Blur Interpolation Transformer for Real-World Motion from Blur. In Proceedings of the Proceedings of the IEEE/CVF Conference on Computer Vision and Pattern Recognition, 2023, pp. 5713–5723.
106. Zou, Y.; Ma, Y. Edgeformer: Edge-Enhanced Transformer for High-Quality Image Deblurring. In Proceedings of the 2023 IEEE International Conference on Multimedia and Expo (ICME). IEEE, 2023, pp. 504–509.
107. Wu, Y.; Lei, L.; Ling, S.; Gao, Z. Hierarchical Patch Aggregation Transformer For Motion Deblurring **2023**.
108. Liang, P.; Jiang, J.; Liu, X.; Ma, J. Image Deblurring by Exploring In-depth Properties of Transformer. *arXiv preprint arXiv:2303.15198* **2023**.
109. Dosovitskiy, A.; Beyer, L.; Kolesnikov, A.; Weissenborn, D.; Zhai, X.; Unterthiner, T.; Dehghani, M.; Minderer, M.; Heigold, G.; Gelly, S.; et al. An image is worth 16x16 words: Transformers for image recognition at scale. *arXiv preprint arXiv:2010.11929* **2020**.
110. Li, H.; Zhao, J.; Zhou, S.; Feng, H.; Li, C.; Loy, C.C. Adaptive Window Pruning for Efficient Local Motion Deblurring. *arXiv preprint arXiv:2306.14268* **2023**.
111. Yan, Q.; Gong, D.; Wang, P.; Zhang, Z.; Zhang, Y.; Shi, J.Q. SharpFormer: Learning Local Feature Preserving Global Representations for Image Deblurring. *IEEE Transactions on Image Processing* **2023**.
112. Köhler, R.; Hirsch, M.; Mohler, B.; Schölkopf, B.; Harmeling, S. Recording and playback of camera shake: Benchmarking blind deconvolution with a real-world database. In Proceedings of the Computer Vision–ECCV 2012: 12th European Conference on Computer Vision, Florence, Italy, October 7–13, 2012, Proceedings, Part VII 12. Springer, 2012, pp. 27–40.
113. Shen, Z.; Wang, W.; Lu, X.; Shen, J.; Ling, H.; Xu, T.; Shao, L. Human-aware motion deblurring. In Proceedings of the Proceedings of the IEEE/CVF International Conference on Computer Vision, 2019, pp. 5572–5581.
114. Jiang, Z.; Zhang, Y.; Zou, D.; Ren, J.; Lv, J.; Liu, Y. Learning event-based motion deblurring. In Proceedings of the Proceedings of the IEEE/CVF Conference on Computer Vision and Pattern Recognition, 2020, pp. 3320–3329.
115. Rim, J.; Lee, H.; Won, J.; Cho, S. Real-world blur dataset for learning and benchmarking deblurring algorithms. In Proceedings of the Computer Vision–ECCV 2020: 16th European Conference, Glasgow, UK, August 23–28, 2020, Proceedings, Part XXV 16. Springer, 2020, pp. 184–201.
116. Rim, J.; Kim, G.; Kim, J.; Lee, J.; Lee, S.; Cho, S. Realistic blur synthesis for learning image deblurring. In Proceedings of the European Conference on Computer Vision. Springer, 2022, pp. 487–503.
117. Li, H.; Zhang, Z.; Jiang, T.; Luo, P.; Feng, H.; Xu, Z. Real-world deep local motion deblurring. In Proceedings of the Proceedings of the AAAI Conference on Artificial Intelligence, 2023, Vol. 37, pp. 1314–1322.
118. Li, L.; Pan, J.; Lai, W.S.; Gao, C.; Sang, N.; Yang, M.H. Learning a discriminative prior for blind image deblurring. In Proceedings of the Proceedings of the IEEE Conference on Computer Vision and Pattern Recognition, 2018, pp. 6616–6625.
119. Liu, Y.; Pu, H.; Sun, D.W. Efficient extraction of deep image features using convolutional neural network (CNN) for applications in detecting and analysing complex food matrices. *Trends in Food Science & Technology* **2021**, *113*, 193–204.

120. Tian, C.; Fei, L.; Zheng, W.; Xu, Y.; Zuo, W.; Lin, C.W. Deep learning on image denoising: An overview. *Neural Networks* **2020**, *131*, 251–275.
121. Rusch, T.K.; Mishra, S. Unicorinn: A recurrent model for learning very long time dependencies. In Proceedings of the International Conference on Machine Learning, PMLR, 2021, pp. 9168–9178.
122. Cui, Q.; Sun, H.; Kong, Y.; Zhang, X.; Li, Y. Efficient human motion prediction using temporal convolutional generative adversarial network. *Information Sciences* **2021**, *545*, 427–447.
123. Gao, H.; Tao, X.; Shen, X.; Jia, J. Dynamic scene deblurring with parameter selective sharing and nested skip connections. In Proceedings of the Proceedings of the IEEE/CVF Conference on Computer Vision and Pattern Recognition, 2019, pp. 3848–3856.
124. Li, L.; Pan, J.; Lai, W.S.; Gao, C.; Sang, N.; Yang, M.H. Dynamic scene deblurring by depth guided model. *IEEE Transactions on Image Processing* **2020**, *29*, 5273–5288.
125. Wan, S.; Tang, S.; Xie, X.; Gu, J.; Huang, R.; Ma, B.; Luo, L. Deep convolutional-neural-network-based channel attention for single image dynamic scene blind deblurring. *IEEE Transactions on Circuits and Systems for Video Technology* **2020**, *31*, 2994–3009.
126. Zou, W.; Jiang, M.; Zhang, Y.; Chen, L.; Lu, Z.; Wu, Y. Sdwnet: A straight dilated network with wavelet transformation for image deblurring. In Proceedings of the Proceedings of the IEEE/CVF International Conference on Computer Vision, 2021, pp. 1895–1904.
127. Kim, K.; Lee, S.; Cho, S. Mssnet: Multi-scale-stage network for single image deblurring. In Proceedings of the European Conference on Computer Vision. Springer, 2022, pp. 524–539.
128. Chen, L.; Lu, X.; Zhang, J.; Chu, X.; Chen, C. Hinet: Half instance normalization network for image restoration. In Proceedings of the Proceedings of the IEEE/CVF Conference on Computer Vision and Pattern Recognition, 2021, pp. 182–192.
129. Tsai, F.J.; Peng, Y.T.; Tsai, C.C.; Lin, Y.Y.; Lin, C.W. Banet: a blur-aware attention network for dynamic scene deblurring. *IEEE Transactions on Image Processing* **2022**, *31*, 6789–6799.
130. Cui, Y.; Ren, W.; Yang, S.; Cao, X.; Knoll, A. Irnnext: Rethinking convolutional network design for image restoration **2023**.
131. Hoßfeld, T.; Heegaard, P.E.; Varela, M.; Möller, S. QoE beyond the MOS: an in-depth look at QoE via better metrics and their relation to MOS. *Quality and User Experience* **2016**, *1*, 1–23.
132. Ruan, L.; Bemana, M.; Seidel, H.p.; Myszkowski, K.; Chen, B. Revisiting Image Deblurring with an Efficient ConvNet. *arXiv preprint arXiv:2302.02234* **2023**.
133. Zhong, Z.; Gao, Y.; Zheng, Y.; Zheng, B.; Sato, I. Real-world video deblurring: A benchmark dataset and an efficient recurrent neural network. *International Journal of Computer Vision* **2023**, *131*, 284–301.
134. Nah, S.; Son, S.; Lee, K.M. Recurrent neural networks with intra-frame iterations for video deblurring. In Proceedings of the Proceedings of the IEEE/CVF Conference on Computer Vision and Pattern Recognition, 2019, pp. 8102–8111.
135. Zhu, C.; Dong, H.; Pan, J.; Liang, B.; Huang, Y.; Fu, L.; Wang, F. Deep recurrent neural network with multi-scale bi-directional propagation for video deblurring. In Proceedings of the Proceedings of the AAAI Conference on Artificial Intelligence, 2022, Vol. 36, pp. 3598–3607.
136. Xiao, J.; Fu, X.; Wu, F.; Zha, Z.J. Stochastic window transformer for image restoration. *Advances in Neural Information Processing Systems* **2022**, *35*, 9315–9329.
137. Su, J.; Xu, B.; Yin, H. A survey of deep learning approaches to image restoration. *Neurocomputing* **2022**, *487*, 46–65.
138. Li, C. A survey on image deblurring. *arXiv preprint arXiv:2202.07456* **2022**.
139. Wang, Z.; Bovik, A.C.; Sheikh, H.R.; Simoncelli, E.P. Image quality assessment: from error visibility to structural similarity. *IEEE Transactions on Image Processing* **2004**, *13*, 600–612.
140. Hore, A.; Ziou, D. Image quality metrics: PSNR vs. SSIM. In Proceedings of the 2010 20th International Conference on Pattern Recognition. IEEE, 2010, pp. 2366–2369.
141. Tu, Z.; Talebi, H.; Zhang, H.; Yang, F.; Milanfar, P.; Bovik, A.; Li, Y. Maxim: Multi-axis mlp for image processing. In Proceedings of the Proceedings of the IEEE/CVF Conference on Computer Vision and Pattern Recognition, 2022, pp. 5769–5780.
142. Mao, X.; Liu, Y.; Liu, F.; Li, Q.; Shen, W.; Wang, Y. Intriguing findings of frequency selection for image deblurring. In Proceedings of the Proceedings of the AAAI Conference on Artificial Intelligence, 2023, Vol. 37, pp. 1905–1913.
143. Zheng, S.; Wu, Y.; Jiang, S.; Lu, C.; Gupta, G. Deblur-yolo: Real-time object detection with efficient blind motion deblurring. In Proceedings of the 2021 International Joint Conference on Neural Networks (IJCNN). IEEE, 2021, pp. 1–8.
144. Wu, A.; Chen, D.; Deng, C. Deep Feature Deblurring Diffusion for Detecting Out-of-Distribution Objects. In Proceedings of the Proceedings of the IEEE/CVF International Conference on Computer Vision, 2023, pp. 13381–13391.
145. Zhao, W.; Hu, G.; Wei, F.; Wang, H.; He, Y.; Lu, H. Attacking Defocus Detection With Blur-Aware Transformation for Defocus Deblurring. *IEEE Transactions on Multimedia* **2023**.
146. Pan, J.; Hu, Z.; Su, Z.; Lee, H.Y.; Yang, M.H. Soft-segmentation guided object motion deblurring. In Proceedings of the Proceedings of the IEEE Conference on Computer Vision and Pattern Recognition, 2016, pp. 459–468.
147. Luo, B.; Cheng, Z.; Xu, L.; Zhang, G.; Li, H. Blind image deblurring via superpixel segmentation prior. *IEEE Transactions on Circuits and Systems for Video Technology* **2021**, *32*, 1467–1482.
148. Zhang, H.; Zhang, J.; Koniusz, P. Few-shot learning via saliency-guided hallucination of samples. In Proceedings of the Proceedings of the IEEE/CVF Conference on Computer Vision and Pattern Recognition, 2019, pp. 2770–2779.
149. Chi, Z.; Wang, Y.; Yu, Y.; Tang, J. Test-time fast adaptation for dynamic scene deblurring via meta-auxiliary learning. In Proceedings of the Proceedings of the IEEE/CVF Conference on Computer Vision and Pattern Recognition, 2021, pp. 9137–9146.

150. Yang, X.; Yu, Z.; Jiang, P.; Xu, L.; Hu, J.; Wu, L.; Zou, B.; Zhang, Y.; Zhang, J. Deblurring Ghost Imaging Reconstruction Based on Underwater Dataset Generated by Few-Shot Learning. *Sensors* **2022**, *22*, 6161.
151. Ren, M.; Delbracio, M.; Talebi, H.; Gerig, G.; Milanfar, P. Multiscale structure guided diffusion for image deblurring. In Proceedings of the Proceedings of the IEEE/CVF International Conference on Computer Vision, 2023, pp. 10721–10733.
152. Whang, J.; Delbracio, M.; Talebi, H.; Saharia, C.; Dimakis, A.G.; Milanfar, P. Deblurring via stochastic refinement. In Proceedings of the Proceedings of the IEEE/CVF Conference on Computer Vision and Pattern Recognition, 2022, pp. 16293–16303.
153. Zhao, S.; Zhang, Z.; Hong, R.; Xu, M.; Zhang, H.; Wang, M.; Yan, S. Crnet: Unsupervised color retention network for blind motion deblurring. In Proceedings of the Proceedings of the 30th ACM International Conference on Multimedia, 2022, pp. 6193–6201.